Published in final edited form as:
Biochemistry. 2012 June 5; 51(22): 4518–4540. doi:10.1021/bi3000287.

Heterotropic Cooperativity within and between Protomers of an Oligomeric M_2 Muscarinic Receptor

Rabindra V. Shivnaraine[†], **Xi-Ping Huang**[‡,§], **Margaret Seidenberg**[‡], **John Ellis**[*,‡], and **James W. Wells**[*,†]

[†]Department of Pharmaceutical Sciences, Leslie Dan Faculty of Pharmacy, University of Toronto, Toronto, Ontario M5S 3M2

[‡]Departments of Psychiatry and Pharmacology, Hershey Medical Center, Penn State University College of Medicine, Hershey, PA 17033

Abstract

At least four allosteric sites have been found to mediate the dose-dependent effects of gallamine on the binding of [^{3}H]quinuclidinylbenzilate (QNB) and *N*-[^{3}H]methylscopolamine (NMS) to M_2 muscarinic receptors in membranes and solubilized preparations from porcine atria, CHO cells, and *Sf*9 cells. The rate of dissociation of [^{3}H]QNB was affected in a bell-shaped manner with at least one Hill coefficient (n_H) greater than 1, indicating that at least three allosteric sites are involved. Binding of [^{3}H]QNB was decreased in a biphasic manner, revealing at least two allosteric sites; binding of [^{3}H]NMS was affected in a triphasic, serpentine manner, revealing at least three sites, and values of n_H greater than 1 pointed to at least four sites. Several lines of evidence indicate that all effects of gallamine were allosteric in nature and observable at equilibrium. The rates of equilibration and dissociation suggest that the receptor was predominately oligomeric, and the heterogeneity revealed by gallamine can be attributed to differences in its affinity for the constituent protomers of a tetramer. Those differences appear to arise from inter- and intramolecular cooperativity between gallamine and the radioligand.

Muscarinic cholinergic receptors contain two topographically distinct sites: an orthosteric site that binds agonists and regulates signaling, and an allosteric site that binds modulators such as gallamine and alcuronium (1). The orthosteric site is located within the cluster of seven transmembrane helices, as in other G protein-coupled receptors of family A, and it is highly conserved among the five muscarinic subtypes (2). The allosteric site is located at the surface between extracellular loops 2 and 3 (2); it is less conserved than the orthosteric site, and allosteric ligands therefore tend to exhibit greater selectivity among the different

[*]James W. Wells, Address: Leslie Dan Faculty of Pharmacy, University of Toronto 144 College Street, Toronto, Ontario, Canada M5S 3M2. jwells@phm.utoronto.ca. Phone: (416) 978-3068. Fax: (416) 978-8511; John Ellis, Address: Department of Psychiatry H073, Penn State University College of Medicine, 500 University Drive, Hershey, PA 17033. johnellis@psu.edu. Phone: (717) 531-4241. Fax: (717) 531-1578.
[§]Current address: Department of Pharmacology, University of North Carolina at Chapel Hill, Chapel Hill, NC 27599

Supporting Information: Theoretical framework and simulated data pertaining to kinetically explicit models of cooperativity in monomeric and dimeric receptors (Equations S1–S14; Figures S1, S2, S16, S17; Tables S12–S15), simulated modulation of the dissociation of an orthosteric probe from a monomeric receptor (Figure S5, Table S2), binding and dissociation of [^{3}H]NMS and [^{3}H]QNB (Figure S3 and S4, Tables S1 and S3), effect of gallamine on the dissociation of [^{3}H]NMS and [^{3}H]QNB under various conditions (Figures S6–S8, Tables S4–S6), effect of gallamine on the apparent affinity of [^{3}H]QNB (Figure S9), dissection of serpentine binding profiles (Figure S10), stabilizing effect of gallamine (Figure S11), effect of gallamine on the binding of [^{3}H]NMS to membrane-bound (Figures S12–S14; Tables S7–S9, S11) and solubilized receptor (Figure S15, Table S10) under various conditions, pseudo-mechanistic analysis of the effect of gallamine on the binding of [^{3}H]NMS prior to the attainment of equilibrium (Equation S15, Figure S18, Table S16). This material is available free of charge via the Internet at http://pubs.acs.org.

Notes: The authors declare no competing financial interests

subtypes (3). The two sites are linked such that binding of a ligand to one affects binding to the other through a process of heterotropic cooperativity. Such effects and the comparative selectivity of the allosteric site have encouraged studies into allosteric ligands as a novel mode of targeted therapeutic intervention (4). The prevalence of allosteric sites within the broader family of GPCRs is unclear, but the purinergic, chemokine, dopaminergic, and serotonergic receptors all have been reported to bind and respond to allosteric ligands in a manner analogous to that of muscarinic receptors and gallamine (1).

GPCRs traditionally have been thought to exist and function as monomers (5). Some GPCRs have been shown to activate G proteins when reconstituted as monomers in size-selective nanodiscs (6-8), and the fluorescence intensities of particles identified by total internal reflection fluorescence microscopy have suggested that monomers are the predominant form of M_1 muscarinic and formyl peptide receptors expressed in CHO cells (9;10). In contrast, much evidence suggests that most if not all GPCRs exist and function as oligomers within complexes that comprise multiple copies not only of the receptor but also of the G protein and perhaps the effector (11-13). Although the oligomer of receptors often is referred to as a dimer, the common methods of detection seldom distinguish between dimers and larger oligomers (*e.g.*, (14;15)). More discerning methods have identified species that are at least trimers (16-18) or tetramers (19-24).

GPCRs of family A also exhibit a characteristic, guanylyl nucleotide-sensitive dispersion of affinities in the binding of agonists. In the case of the M_2 muscarinic receptor, those effects can be described quantitatively in terms of cooperative interactions among the four orthosteric sites of a tetramer (19;22). Since the breadth of the dispersion is a measure of efficacy (25;26), such agreement implies that cooperativity is involved in the mechanism whereby the receptor recognizes the agonist and relays the signal to downstream effectors. Cooperativity among four protomers of the M_2 receptor also can account for noncompetitive effects in the binding of the antagonists *N*-methylscopolamine and quinuclidinylbenzilate (22;27;28).

The gallamine-specific site on the M_2 receptor is the most studied allosteric site of any GPCR (29), yet the implications of an oligomer for heterotropic effects generally have been disregarded. If the oligomeric nature of the system were sensed by an allosteric ligand, two forms of heterotropic cooperativity can be envisaged: intramolecular cooperativity between allosteric and orthosteric ligands on the same protomer (3;30), and intermolecular cooperativity between ligands on different protomers. A tetrameric receptor would possess a total of eight sites—four orthosteric and four allosteric—and potentially could host 16 different heterotropic interactions. The number of interactions is increased further by the possibility of homotropic cooperativity between orthosteric sites, allosteric sites, or both.

The present investigation was prompted by two reports in which an allosteric ligand appeared to recognize at least two sites at the M_2 receptor. In the first, the Hill coefficient was shown to exceed 1 for the effect of tacrine on the rate of dissociation of *N*-[^{3}H]methylscopolamine and on its binding at thermodynamic equilibrium (31). In the second, the rate of dissociation of [^{3}H]quinuclidinylbenzilate was increased and decreased in a bell-shaped manner at graded concentrations of gallamine (32). We have reproduced the complex effect of gallamine on the dissociation of [^{3}H]quinuclidinylbenzilate and show that more than two sites are involved. We also show that gallamine affects the binding of *N*-[^{3}H]methylscopamine in a triphasic, serpentine manner indicative of at least four sites. Essentially the same patterns have been found with M_2 receptor from different sources, both in membranes and after extraction in digitonin–cholate.

The data can be rationalized in terms of a receptor that is at least tetrameric. Within that complex, a mix of homotropic and heterotropic interactions determines the binding of gallamine and its allosteric effects at orthosteric sites on the same and neighboring protomers. This interpretation recognizes the oligomeric nature of the receptor, in contrast to the common view in which all effects of gallamine are ascribed to one or more sites on a single protomer. The results illustrate the scope for cooperativity within oligomers of GPCRs and argue for a reassessment of heterotropic interactions in those that possess an allosteric site (1;33;34).

EXPERIMENTAL PROCEDURES

Ligands, Detergents, and other Materials

N-[^{3}H]Methylscopolamine was obtained as the chloride salt from PerkinElmer (lots 3406081 and 3474009, 83.5 Ci/mmol; 3436143, 3499213 and 3538031, 81.0 Ci/mmol) and as the bromide salt from Amersham Biosciences (batches B-32, 84.0 Ci/mmol; B-35, B-36, 81.0 Ci/mmol and B-38, 80 Ci/mmol). Mass spectra provided by the manufacturer indicated that the samples were devoid of contaminating scopolamine. (−) -[^{3}H]Quinuclidinylbenzilate was purchased from PerkinElmer (lots 3363717, 37.0 Ci/mmol, 3467373, 39 Ci/mmol; 3499844, 42.0 Ci/mmol) and Amersham (batches B-49, 49.0 Ci/mmol; B-50, 41 Ci/mmol). Both radioligands were supplied as a solution in ethanol, which was removed by evaporation prior to use. Atropine sulfate (Batches 69H0545 and 88H0122) and gallamine triethiodide (batches 115K1554 and 033K1443) were obtained from Sigma-Aldrich.

The protease inhibitors bacitracin, leupeptin, pepstatin A, and benzamidine were obtained from Sigma-Aldrich, and Complete Protease Inhibitor Cocktail tablets were from Roche. Protein was estimated by means of bicinchoninic acid using the BCA Protein Assay Kit from Pierce, with bovine serum albumin from Sigma taken as the standard. Digitonin used to solubilize the receptor was purchased from Wako Chemicals USA at a purity near 100%; that used to prepare and elute the columns of Sephadex G-50 in the binding assays was from Calbiochem. Sodium cholate was purchased from Sigma-Aldrich at purity of at least 99%. HEPES was obtained as the free base from Boehringer Mannheim, and EDTA was obtained as the disodium salt from Sigma-Aldrich. Other chemicals were obtained as described below or from sources identified previously (22).

Polypropylene columns used in the binding assays were obtained from Kontes (Disposaflex, 0.8 × 6.5 cm) and were packed with Sephadex G-50 from Sigma-Aldrich. Fiberglass filters used in the binding assays were from Whatman Schleicher and Schuell (No. 32).

Muscarinic Receptor from Porcine Atria

The M_2 receptor is the predominant muscarinic subtype in porcine atria, from which it was prepared as described previously (28). Briefly, atria were collected immediately after slaughter, taking care to avoid the sinus and atrioventricular nodes. The tissue was washed twice with ice-cold PBS (20 mM KH_2PO_4, 150 mM NaCl, NaOH to pH 7.40) and homogenized in buffer A (20 mM imidazole, 1 mM EDTA, 0.1 mM PMSF, 0.02% NaN_3, HCl to pH 7.60) supplemented with benzamidine (1 mM), pepstatin A (20 μg/mL), leupeptin (0.2 μg/mL), and bacitracin (200 μg/mL). The resulting homogenate was fractionated by centrifugation on a sucrose density gradient (13–28%) to obtain the sarcolemmal fraction, which then was centrifuged for 45 min at 4 °C and 100,000 × *g*. The pellet was resuspended in buffer A or buffer B (20 mM HEPES, 1 mM EDTA, 0.1 mM PMSF, NaOH to pH 7.40) and assayed for binding at a saturating concentration of [^{3}H]quinuclidinylbenzilate. Samples in buffer A were centrifuged for 45 min at 4 °C and

100,000 × *g*, and the pellets were stored at −75 °C until required for further treatment as described below. Samples in buffer B were divided into aliquots and centrifuged for 10 min at 4 °C and 18,000 × *g*, and the pellets were stored at −75 °C until required for binding assays.

Atrial membranes were depleted of cholesterol by means of methyl-β-cyclodextrin (35). The sarcolemmal fraction from sucrose density gradients was thawed and resuspended in buffer A, to which methyl-β-cyclodextrin was added at a final concentration of 100 g/L. The final concentration of total protein was 1.5 g/L. The suspension was shaken for 3 h at room temperature and centrifuged for 45 min at 4 °C and 100,000 × *g*, and the resulting pellets were stored at −75 °C until required for binding assays. The amount of cholesterol in native and cholesterol-depleted membranes was quantified using a cholesterol assay kit from BioVision (35).

To solubilize the receptor from porcine atria, the sarcolemmal fraction from sucrose density gradients was thawed and resuspended in buffer A supplemented with digitonin (0.36%) and cholate (0.08%). The concentration of protein was 5.5 g/L. The mixture was incubated for 10 min at 24 °C and centrifuged for 45 min at 4 °C and 100,000 × *g* to obtain a pellet that was resuspended in buffer A supplemented with digitonin (0.8%) and cholate (0.08%). The mixture then was shaken for 10 min at room temperature, diluted to 0.4% digitonin with an equal volume of buffer A, and centrifuged for 45 min at 4 °C and 100,000 × *g*. The supernatant containing the solubilized receptor was divided into aliquots and stored at −75 °C until required for binding assays. Further details have been described previously (27;28;36;37).

M_2 Muscarinic Receptor from CHO and *Sf*9 Cells

CHO cells stably expressing the human M_2 receptor were maintained at 37 °C, 5% CO_2, and 100% humidity in F-12 media (Sigma-Aldrich) supplemented with fetal bovine serum (5%), penicillin (100 units/mL), and streptomycin (100 μg/mL). The cells were harvested and homogenized in ice-cold 5 mM phosphate buffer (1 mM KH_2PO_4, 4 mM Na_2HPO_4, pH 7.4) with three pulses (15 s) of a Bio Homogenizer (Biospec Products, Inc., Bartlesville, OK), and the mixture was centrifuged for 30 min at 4 °C and 50,000 × g. The pellet was resuspended in ice-cold 5 m M phosphate buffer, divided into aliquots, and stored at −70 °C. Further details have been described previously (38).

*Sf*9 cells coexpressing human M_2 receptors tagged at the *N*-terminus with either the c-Myc or the FLAG epitope were prepared as described previously (39). The cells were cultured at 27 °C in Ex-Cell 400 insect media (JRH Biosciences) containing fetal bovine serum albumin (2%), Fungizone (1%), and gentamycin (0.1%) (Life Technologies, Gibco-BRL) and grown to confluence at a density of 2×10^6 cell/mL. When in log phase of growth, the cells were coinfected with equivalent titres of the two baculoviruses at a total multiplicity of infection of 5 plaque-forming units per cell. They were harvested 48 h after infection, collected by centrifugation for 15 min at 4 °C and 1,000 × *g*, and stored at −75 °C.

Harvested *Sf*9 cells were homogenized and washed twice in buffer D (20 mM KH_2PO_4, 20 mM NaCl, 1 mM EDTA, 0.1 mM PMSF, Complete Protease Inhibitor tablets, NaOH to pH 7.4) by centrifugation for 45 min at 4 °C and 100,000 × *g*. Receptor was extracted from the washed membranes in digitonin–cholate (0.86% digitonin, 0.17% cholate) as described previously (40). The solubilized product was divided into aliquots and stored at −75 °C. To prepare samples for binding assays, washed membranes were resuspended in buffer B, divided into aliquots, and centrifuged for 10 min at 4 °C and 18,000 × *g*. The resulting pellets were stored at −75 °C.

Binding Assays

Assays were performed in buffer B except where stated otherwise. Magnesium-free buffers of comparatively low ionic strength are optimal for detecting the allosteric effects of gallamine at the M_2 receptor (41). For studies on detergent-solubilized extracts, buffer B was supplemented with 0.1% digitonin and 0.02% cholate. Ligands to be mixed with the receptor were dissolved in buffer B or other buffer as required for the assay.

The rate of dissociation of a radioligand from membrane-bound M_2 receptor was measured by two-point assays as described previously (32). Membranes were suspended in buffer solution at a protein concentration of 2–5 μg/mL, and aliquots of the mixture (1 mL) were incubated with *N*-[^{3}H]methylscopolamine for 30 min at 24 °C or with [^{3}H]quinuclidinylbenzilate for 60 min at 37 °C. Net dissociation of the radioligand was initiated by the addition of atropine (3 μM in a final volume of 2 mL), either alone or together with gallamine at the required concentration. After further incubation for the specified time, the reaction was terminated by filtration of the sample through fibreglass filters pre-treated with a solution of polyethylenimine (0.1%) in water. The filters then were washed twice with 5 mL of ice-cold 40 mM phosphate buffer (8 mM KH_2PO_4, 32 mM Na_2HPO_4, pH 7.4) and assayed for radioactivity as described below.

To measure the rate of dissociation of *N*-[^{3}H]methylscopolamine or [^{3}H]quinuclidinylbenzilate from solubilized M_2 receptor, an aliquot of the radioligand dissolved in buffer B was placed in a polypropylene microcentrifuge tube (2 mL) and mixed with the receptor in the ratio 50:3 (v/v). The radioligand was present at a final concentration near its equilibrium dissociation constant unless otherwise indicated (*N*-[^{3}H]methylscopolamine, K_D = 10 nM; [^{3}H]quinuclidinylbenzilate, K_D = 1 nM; Figure S3A and Table S1). The reaction mixture was incubated for 45 min (*N*-[^{3}H]methylscopolamine) or 2 h ([^{3}H]quinuclidinylbenzilate), and three aliquots (50 μL each) were removed to determine the level of initial binding (*i.e.*, t = 0). Net dissociation of the radioligand then was initiated by the addition of atropine at a final concentration of 3 μM; dilution of the receptor at this step was negligible (< 0.02%). The concentration of atropine was sufficient to block reassociation at all orthosteric sites (Figure S3B and Table S1) without affecting binding to the allosteric site (42). Following the addition of atropine, aliquots of the reaction mixture (50 μL) were removed in duplicate at times up to 3 min and in triplicate thereafter. Bound radioligand was separated by applying each aliquot to a column of Sephadex G-50 Fine (0.8 × 6.5 cm) pre-equilibrated with buffer C (20 mM HEPES, 1 mM EDTA, NaOH to pH 7.40) supplemented with digitonin (0.017%). Further details regarding the separation have been described previously (22).

Various preparations and conditions were examined for the dose-dependent effect of gallamine on the binding of *N*-[^{3}H]methylscopolamine or [^{3}H]quinuclidinylbenzilate at selected concentrations of the radioligand. Some studies involved a comparison of several binding profiles obtained at different times over a period of incubation during which there was a time-dependent loss of receptor at lower concentrations of gallamine. In such cases, the profiles were acquired in groups of two or three measured at different times in order to track the relationship over time between one profile and another.

For studies on membranes from porcine atria, *Sf*9 cells, or CHO cells, frozen samples were thawed and resuspended in the required buffer solution by means of a Potter-Elvehjem tissue-homogenizer. The final concentration of total protein was 2–5 μg/mL. Aliquots of the homogenate (1 mL) then were mixed with the radioligand alone, the radioligand plus gallamine, or the radioligand plus atropine according to one of two protocols that differed in the order of mixing. In the first protocol, *N*-[^{3}H]methylscopolamine and gallamine were premixed at the required concentration of the latter; the receptor then was added to the

ligands (20 μL), and the mixture was incubated for the specified time at 25 °C prior to the measurement of binding. In the second, *N*-[^{3}H]methylscopolamine (10 μL) was added to the receptor alone and incubated for 30 min at 25 °C; gallamine (10 μL) then was added at the required concentration, and incubation was continued at 25 °C for the specified time prior to the measurement of binding. The reaction was terminated by passage of the sample through a fiberglass filter mounted on a Brandel cell harvester. Nonspecific binding was taken throughout as that in the presence of atropine (3 μM), which was premixed with *N*-[^{3}H]methylscopolamine prior to the addition of receptor. Other details have been described previously (43).

For studies on solubilized receptor from porcine atria or *Sf*9 cells, aliquots of the extract (3 μL) were added to polypropylene microcentrifuge tubes (0.5 mL) containing the required ligands dissolved in buffer B (50 μL): namely, the radioligand alone, gallamine alone, the radioligand plus gallamine, or the radioligand plus atropine. Receptor and ligands were mixed according to the two protocols described above except that incubation was at 30 °C throughout. In a third protocol, the receptor was mixed first with gallamine and incubated for 2 h at 30 °C; an aliquot of the radioligand then was added, and incubation was continued for the specified time. To terminate the reaction, an aliquot of the mixture (50 μL) was applied to a column of Sephadex G-50 and processed as described above. Assays were performed in triplicate, and nonspecific binding was taken throughout as that in the presence of atropine (30 μM).

To measure the level of radioactivity, each sample was counted twice for 5 min by liquid scintillation spectrometry (Beckman LS7800, Beckman LS6500 or Packard 2100TR). The background was subtracted, and the rate of disintegration (dpm) was determined from the counting efficiency as estimated by means of quenched standards. Individual estimates of dpm from replicate samples counted twice were averaged to obtain the mean and standard error used in subsequent analyses.

Analysis of Data

The net dissociation of *N*-[^{3}H]methylscopolamine or [^{3}H]quinuclidinylbenzilate over time was analyzed in terms of a single exponential according to Equation 1, in which B_{obsd} is the total binding of the radioligand at time t, k_{obsd} is the rate constant, and $B_{t=0}$ and $B_{t\to\infty}$ represent the initial and asymptotic levels of binding, respectively. The fits were not improved by the addition of a second exponential ($P > 0.05$).

$$B_{obsd}=(B_{t=0} - B_{t\to\infty})e^{-k_{obsd}t}+B_{t\to\infty} \quad (1)$$

Time-courses at one or more concentrations of gallamine were accompanied in the same experiment by a control from which the allosteric ligand was omitted. The data from all traces were analyzed in concert with a single value of $B_{t\to\infty}$, a constraint that was without appreciable effect on the sum of squares ($P > 0.05$). Each individual time-course within the analysis was assigned separate values of k_{obsd} and $B_{t=0}$. The value of k_{obsd} in the absence of gallamine was designated k_0, and each value of k_{obsd} in the presence of gallamine was normalized with respect to k_0 from the same experiment to obtain the ratio k_{obsd}/k_0 for subsequent analyses.

Binding at graded concentrations of *N*-[^{3}H]methylscopolamine or [^{3}H]quinuclidinylbenzilate was analyzed in terms of Equation 2, in which B_{max} represents maximal specific binding of the radioligand (P); B_{obsd} and B_{sp} represent total and specific binding, respectively, at the total concentration $[P]_t$. The parameter K is the concentration of unbound radioligand that corresponds to half-maximal specific binding, and n_H is the Hill

coefficient; *NS* is the fraction of unbound radioligand that appears as nonspecific binding. Equation 2 was solved numerically as described previously (44).

$$B_{obsd}=B_{max}\frac{([P]_t-B_{sp})^{n_H}}{K^{n_H}+([P]_t-B_{sp})^{n_H}}+NS([P]_t-B_{sp}) \quad (2)$$

The inhibitory effect of atropine on the specific binding of *N*-[^{3}H]methylscopolamine was analyzed according to Scheme 1, in which a radioligand (P) and an unlabeled ligand (A) compete for a uniform population of mutually independent sites. The parameters K_P and K_A represent the equilibrium dissociation constants of P and A, respectively.

Scheme 1 was formulated as the equation $B_{obsd} = [P][R]_t/\{[P] + K_P(1 + [A]/K_A)\} + NS[P]$, where [A] and [P] are the free concentrations of the two ligands, and $[R]_t$ is the total concentration of receptor. When binding led to appreciable depletion, the values of [A] and [P] were computed numerically from the total concentrations as described previously (44).

Dose-dependent effects of gallamine (G) on the rate of dissociation of *N*-[^{3}H]methylscopolamine or [^{3}H]quinuclidinylbenzilate (k_{obsd}/k_0), or on the level of total binding at a specified time (B_{obsd}), were analyzed empirically in terms of Equation 3.

$$Y_{obsd}=Y_{[G]\to\infty}+(Y_{[G]=0}-Y_{[G]\to\infty})\sum_{j=1}^{n}\frac{F_jK_j^{n_{H(j)}}}{[G]_t^{n_{H(j)}}+K_j^{n_{H(j)}}} \quad (3)$$

The variable Y_{obsd} represents the value of k_{obsd}/k_0 or B_{obsd} at the total concentration $[G]_t$ of the allosteric ligand, and the parameters $Y_{[G]=0}$ and $Y_{[G]\to\infty}$ represent the value of Y_{obsd} in the absence of gallamine and at saturating concentrations, respectively. The gallamine-sensitive component of Y is described as a sum of n Hill terms; the difference $Y_{[G]=0} - Y_{[G]\to\infty}$ is the net change effected by gallamine, F_j is the fractional contribution of term j (*i.e.*, $\sum_{j=1}^{n}F_j=1$), $n_{H(j)}$ is the corresponding Hill coefficient, and K_j is the concentration of gallamine that yields a half-maximal signal at fraction *j*.

Most analyses in terms of Equation 3 involved 6–12 sets of data acquired under different conditions with respect to the time of incubation or the concentration of the radioligand. In such cases, each set of data was assigned a separate value of $Y_{[G]=0}$ and $Y_{[G]\to\infty}$. Data from two or more experiments conducted under the same conditions were assigned single values of K_j, F_j, and $n_{H(j)}$. The fitted values of $n_{H(j)}$ obtained in this manner often were similar from one set of conditions to the next. Single values of $n_{H(j)}$ therefore were assigned to all of the data whenever the reduction in parameters could be achieved without a significant increase in the sum of squares ($P > 0.05$). Such constraints on K_j or F_j generally were not tolerated ($P < 0.05$). Further details regarding the assignment of shared parameters are described elsewhere as required.

In some preparations, prolonged incubation of the receptor with *N*-[^{3}H]methylscopolamine and gallamine resulted in a time-dependent loss of sites at lower concentrations of the allosteric ligand. Some analyses in terms of Equation 3 included data pooled from experiments in which the magnitude of the decrease varied from one curve to another. Such losses emerged as a decrease in the fitted value of $Y_{[G]=0}$ and were accommodated further by the assignment of separate values of $n_{H(1)}$ to data acquired under different conditions. Also, the fitted or mapped value of F_3 was adjusted upward according to Equation 4, in which $Y_{[G]=0,stable}$ and $Y_{[G]=0,unstable}$ represent the values of $Y_{[G]=0}$ for binding to the

receptor before and after the loss of sites, respectively; the constant $F_{3,max}$ represents the value of F_3 at equilibrium and was determined as described below.

$$F_3 = F_{3,max} \frac{Y_{[G]=0,stable}}{Y_{[G]=0,unstable}} \quad (4)$$

Scaling and Presentation of Data

Results of analyses involving multiple sets of data from replicated experiments have been presented with reference to a single fitted curve. To obtain the values plotted on the *y*-axis, estimates of observed binding (Y_{obsd}) or specific binding (Y_{sp}) were adjusted according to the equation $Y' = Y\{f(\bar{\mathbf{x}}_i, \bar{\mathbf{a}}) / f(\mathbf{x}_i, \mathbf{a})\}$ (27). The function f represents the fitted model. The vectors $\mathbf{x}_i$ and $\mathbf{a}$ represent the independent variables at point i and the fitted parameters for the set of data under consideration; $\bar{\mathbf{x}}_i$ and $\bar{\mathbf{a}}$ are the corresponding vectors in which values that differ from experiment to experiment have been replaced by the means for all experiments included in the analysis.

In the case of Equation 3 and gallamine, individual estimates of Y_{obsd} were decreased by the value obtained for nonspecific binding in the same experiment (Y_{ns}) to obtain the corresponding estimates of specific binding (*i.e.*, $Y_{sp} = Y_{obsd} - Y_{ns}$). The latter then were normalized as described above to the mean values of $Y_{[G]=0} - Y_{ns}$ and $Y_{[G]\rightarrow\infty} - Y_{ns}$. The resulting values of Y' at the same $\mathbf{x}_i$ were averaged to obtain the mean and standard error for each point plotted in the figure. When the receptor was stable under all conditions represented in the analysis, the mean value of $Y_{[G]=0} - Y_{ns}$ was taken as 100 throughout, and that of $Y_{[G]\rightarrow\infty} - Y_{ns}$ was taken as the corresponding fraction of 100. When there was a time-dependent loss of sites, the mean value of $Y_{[G]=0} - Y_{ns}$ was reduced accordingly. To determine the magnitude of the reduction, experiments were conducted such that assays after different periods of incubation were performed in parallel. The value of $Y_{[G]=0}$ at any time therefore could be compared with that prior to the onset of instability. In such cases, the mean value of $Y_{[G]\rightarrow\infty} - Y_{ns}$ was taken as a percentage of $Y_{[G]=0} - Y_{ns}$ prior to the onset of instability.

Statistical Procedures

All equations were fitted to the data by nonlinear regression (45). Equilibrium constants and potencies were optimized throughout on a logarithmic scale, and rate constants were optimized on a linear scale. The effects of various constraints on the weighted sum of squares were assessed by the means of the *F*-statistic. Weighting of the data and other statistical procedures were performed as described previously (19;44).

Weighted residuals were of comparable magnitude within each set of data, and the individual sets of data in global analyses generally made comparable contributions to the total weighted sum of squares. The fits therefore were not dominated by the data from one experiment or group of experiments. Mean parametric values calculated from independent estimates are presented together with the standard error. For parametric values derived from a single analysis of one or more sets of data, the errors were estimated from the diagonal elements of the covariance matrix at the minimum in the sum of squares.

RESULTS

Binding of Orthosteric Antagonists

The specific binding of *N*-[^{3}H]methylscopolamine and [^{3}H]quinuclidinylbenzilate to M_2 receptor in preparations from porcine atria, *Sf*9 cells, and CHO cells revealed a single class

of sites, as indicated by Hill coefficients indistinguishable from 1 ($P > 0.05$) (Equation 2). The affinities were similar or the same with membranes from all three sources and 40–60-fold weaker in digitonin-solubilized extracts (Table S1). The pattern obtained with *N*-[^{3}H]methylscopolamine in extracts from porcine sarcolemma is illustrated in Figure S3A.

Hill coefficients also were indistinguishable from 1 for the inhibition of *N*-[^{3}H]methylscopolamine at graded concentrations of atropine ($P > 0.05$) (Figure S3B). The affinity of atropine was about 0.4 nM for receptor in membranes and about 30 nM for that in extracts (Table S1), as estimated in terms of Scheme 1. Based on these values, atropine was used at a concentration of 3 μM to block the reassociation of *N*-[^{3}H]methylscopolamine and [^{3}H]quinuclidinylbenzilate in studies on their rates of dissociation from orthosteric sites. Specific binding of the radioligand in assays at graded concentrations of gallamine was taken as that portion of total binding inhibited by 3 μM atropine in the case of membranes and 30 μM atropine in the case of extracts.

Kinetics of Dissociation

A single exponential was sufficient to describe the net dissociation of *N*-[^{3}H]methylscopolamine and [^{3}H]quinuclidinylbenzilate under all conditions with or without gallamine. Typical data are illustrated in Figure S4 for receptor extracted from porcine atria, and similar results have been reported previously for membrane-bound receptor (46). The monoexponential nature of the process when an allosteric ligand and an orthosteric probe are both present requires only that the former dissociate at least threefold faster than the latter (Figure S5 and Table S2).

The observed rate constant for dissociation of either radioligand (k_{obsd}) varied about 1.4-fold among experiments conducted on different occasions but otherwise under identical conditions. For example, the range of values obtained for *N*-[^{3}H]methylscopolamine was 0.179–0.247 min^{-1} with receptor extracted from porcine atria ($N = 6$) and 0.054–0.059 min^{-1} with receptor extracted from *Sf*9 cells ($N = 4$). The range obtained for [^{3}H]quinuclidinylbenzilate was 0.013–0.018 min^{-1} with receptor extracted from porcine atria ($N = 5$). In order to compare the results from different experiments, values of k_{obsd} measured in the presence of gallamine were expressed relative to that measured in its absence (k_0) in the same experiment (*i.e.,* k_{obsd}/k_0) (47).

The dissociation of *N*-[^{3}H]methylscopolamine was slowed at all concentrations of gallamine and in all preparations of receptor (*e.g.*, Figure 1, Figure S4B). The Hill coefficient for the decrease in k_{obsd}/k_0 was indistinguishable from 1 throughout (Table 1) ($P > 0.05$), suggesting a single class of allosteric sites. In contrast, the dissociation of [^{3}H]quinuclidinylbenzilate was hastened by gallamine at lower concentrations ($k_{obsd}/k_0 > 1$) and slowed at higher concentrations ($k_{obsd}/k_0 < 1$) to yield a bell-shaped profile (*e.g.*, Figure 1, Figure S4A). Essentially the same pattern was observed under various conditions with respect to the concentration of the orthosteric probe (Figure 1D, Table 2), ionic composition (Figure S6B, Table S4), DTT (Figure S7, Table S5), and the level of cholesterol (Figure S8, Table S6).

The bell-shaped profile for the effect of gallamine on the dissociation of [^{3}H]quinuclidinylbenzilate could be described as a sum of two Hill terms (Equation 3, $n = 2$). The Hill coefficient associated with each term tended to exceed 1 in atrial preparations (Table 1), and there was a significant increase in the sum of squares when both values of $n_{H(j)}$ were fixed at 1 rather than optimized ($P < 0.05$). It follows that at least one term of Equation 3 is associated with two or more sites for gallamine, suggesting that there are at least three sites overall. The increase in the sum of squares generally was small when the value of only $n_{H(1)}$ or $n_{H(2)}$ was fixed at 1 ($P > 0.05$). It therefore is not clear in such cases

whether apparent cooperativity in the binding of gallamine pertains to the processes that hasten dissociation, slow dissociation, or both.

In the absence of an allosteric ligand, the rate of dissociation of [^{3}H]quinuclidinylbenzilate from membrane-bound receptors was independent of the level of occupancy attained by the radioligand (Table S3). In the presence of gallamine, higher occupancy of the receptor in CHO membranes led to faster dissociation and a corresponding increase in the amplitude of the peak at about 5 μM gallamine (Figure 1D). The increase could be attributed wholly to an increase in the fitted value of F_2 (Equation 3), from 1.5 at 0.02 nM [^{3}H]quinuclidinylbenzilate to 2.2 at 4 nM (Table 2). There was little or no effect of occupancy on the value of $n_{H(j)}$ or K_j at either class of sites, and both parameters could be shared among all of the data without an appreciable change in the sum of squares ($P = 0.8$) (Table 2). If the effect of [^{3}H]quinuclidinylbenzilate on F_2 is described by a single hyperbolic term (Figure S9), the estimated potency of the radioligand is 0.31 nM (log EC_{50} = −9.51). In contrast to CHO membranes, the dissociation of [^{3}H]quinuclidinylbenzilate from receptor in native and cholesterol-depleted sarcolemmal membranes was independent of the concentration of the radioligand irrespective of gallamine (Figure S8, Table S6).

Treatment of *Sf*9 membranes with DTT increased the rate of dissociation of [^{3}H]quinuclidinylbenzilate almost threefold in the absence of an allosteric ligand (Table S3), and the maximal effect of gallamine on k_{obsd}/k_0 was reduced through a decrease in the relative apparent affinity for the two classes of sites (*i.e.,* K_2/K_1) and a concomitant decrease in F_2 (Figure S7, Table S5). A change in the ionic composition of the buffer also affected the effect of gallamine on the dissociation of both *N*-[^{3}H]methylscopolamine and [^{3}H]quinuclidinylbenzilate, at least with receptor in membranes from CHO cells (Figure S6, Table S4). Such effects were comparatively small, however, and they did not alter the bell-shaped nature of the pattern observed with [^{3}H]quinuclidinylbenzilate.

Equilibration of N-[^{3}H]Methylscopolamine and Gallamine with Solubilized M_2 Receptor

The kinetics of dissociation reveal at least two classes of sites for gallamine (Figure 1D). Saturation required concentrations exceeding 100 μM, which markedly slowed the dissociation of *N*-[^{3}H]methylscopolamine. At a concentration of 100 μM, for example, gallamine reduced the value of k_{obsd} about 60-fold, from 1.8×10^{-1} min^{-1} to 3.2×10^{-3} min^{-1}; that in turn increased the time required for equilibration from about 0.33 h to more than 18 h (*i.e.*, $5 \times t_{1/2}$). In light of this, the dose-dependent effect of gallamine on the binding of *N*-[^{3}H]methylscopolamine was measured after periods of incubation that varied from 3 h to 30 h. The longer times greatly exceed the periods of 2–3 h that have been typical of previous studies involving gallamine (*e.g.*, (48;49)).

Binding patterns measured after the simultaneous addition of gallamine and *N*-[^{3}H]methylscopolamine were essentially the same, irrespective of temperature, with receptor extracted from sarcolemmal membranes (4 °C, 30 °C, and 37 °C) and from *Sf*9 cells (30 °C). Development of the pattern over time is illustrated in Figures 2 (atrial extracts) and 3 (*Sf*9 extracts), where about 50% of the sites were occupied by the radioligand. After shorter periods of incubation, the effect of gallamine was biphasic downward (Figure 3A); after more prolonged incubation, the curves became triphasic owing to the appearance of a peak at 100 μM gallamine. Emergence of the serpentine pattern was accompanied by an increase in the asymptotic level of binding at saturating concentrations of gallamine and, in atrial extracts, a decrease in binding at lower concentrations. The pattern developed more rapidly at higher temperatures (Figure 2). It also developed sooner in extracts from atria than in extracts from *Sf*9 cells (cf. Figure 2D and Figure 3C), at least at 30 °C, in accord with the observation that the net dissociation of *N*-[^{3}H]methylscopolamine was faster in the former (Figure 3D, inset).

The data were described empirically in terms of Equation 3 with three terms: one for the decrease in bound *N*-[^{3}H]methylscopolamine at low concentrations of gallamine (1–1,000 nM) ($j = 1$), a second for the increase at intermediate concentrations (1–100 μM) ($j = 2$), and a third for the decrease at the highest concentrations (0.1–10 mM) ($j = 3$). The magnitude of each term is given by the corresponding value of F_j (Figure S10), which is positive for a gallamine-dependent decrease in binding and negative for an increase. The value of F_3 therefore represents a theoretical upper limit on the gallamine-sensitive binding of *N*-[^{3}H]methylscopolamine under the conditions of the assay; in practice, it would be achieved only if the net effect of K_1 and K_2 were not offset by the decrease associated with K_3.

Preliminary analyses indicated that time and other variables affected the values of F_j while having little or no effect on K_j or $n_{H(j)}$. Estimates of K_j, $n_{H(j)}$, and F_j tend to be correlated, however, and data acquired at different times of incubation but under otherwise identical conditions were combined to reduce the total number of parameters. With extracts from porcine atria (Figure 2) and *Sf*9 cells (Figure 3), there is a substantial increase in the weighted sum of squares when data acquired after different times of incubation are assigned single rather than separate values of F_2 and F_3 ($P < 0.001$). There is a similar increase when both K_j and $n_{H(j)}$ are assigned a single value for each j ($P \leq 0.002$) but not when either K_j or $n_{H(j)}$ is constrained separately ($P > 0.05$); in the latter case, effects on the sum of squares and the values of other parameters are smaller with the constraint on $n_{H(j)}$.

These comparisons suggest that the Hill coefficients were insensitive to the time of incubation, and similar results were obtained with other preparations described below. Pooled data therefore were analyzed with common values of $n_{H(j)}$ except where indicated otherwise. After the onset of instability, the value of $n_{H(1)}$ was indistinguishable from 1 ($P > 0.05$) and was fixed accordingly. The fitted curves obtained with these constraints are compared with the data in the different panels of Figures 2 and 3. Those obtained after different periods of incubation are superimposed in panels A (30 °C) and F (37 °C) of Figure 2 and in panel A of Figure 3 (30 °C). The corresponding parametric values are listed in Table 3.

In terms of Equation 3, the emergence of the peak at about 100 μM gallamine is due to a time-dependent increase in the number of sites (F_2) associated with K_2 and a concomitant increase in the value of K_3. The trend is clearest with receptor from *Sf*9 cells, which was stable under all conditions (Figure 3). The binding of *N*-[^{3}H]methylscopolamine in the absence of gallamine was maximal at 6 h of incubation and remained unchanged for at least 15 h thereafter (*i.e.*, $Y_{[G]=0}$ in the inset to Figure 3B). The asymptotic level of binding at saturating concentrations of gallamine increased over time, with most of the change occurring within the first 9 h (*i.e.*, $Y_{[G]\rightarrow\infty}$ in the inset to Figure 3B). It follows that net gallamine-sensitive binding (*i.e.*, $Y_{[G]=0} - Y_{[G]\rightarrow\infty}$) was essentially unchanged between 9 h to 21 h. Over the same period, the value of F_2 decreased from −0.39 to −0.56 with comparatively little change in F_1 (Table 3). The growth of the peak therefore emerges largely as an increase in the intrinsic maximum represented by F_3: that is, from an increase in the number of sites potentially accessible to the radioligand. The amplitude was increased further by a small increase in K_3, from 0.15 mM after 9 h to 0.44 mM after 21 h (Table 3).

With extracts from porcine atria, the pattern is complicated by the time-dependent loss of receptor that occurred at lower concentrations of gallamine. Binding of *N*-[^{3}H]methylscopolamine in the absence of gallamine was maximal after 3 h of incubation at 30 °C, remained unchanged until about 15 h, and then decreased to about 60% of the initial value after 21 h (Figure 2C, inset). A concomitant increase in binding at saturating concentrations of gallamine was complete after 15 h of incubation (Figure 2C, inset). A similar pattern was observed at 37 °C (Figure 2), but the loss of receptor in the absence of

gallamine occurred sooner than at 30 °C (Figure 2D and inset). The loss of receptor therefore contributes to a decrease in the quantity $Y_{[G]=0} - Y_{[G]\rightarrow\infty}$, which in turn affects the corresponding values of F_j.

To examine further the nature of the instability in atrial extracts, aliquots of the same sample were incubated in parallel for 9 h or 21 h at 37 °C, thereby permitting data acquired at different times to be compared in absolute units (Figure S11). Whereas binding at concentrations of gallamine below about 1 μM decreased over time, as seen in the fitted value of $Y_{[G]=0}$ (Figure 2D, inset), the loss became progressively less at higher concentrations and was prevented at concentrations at or above 100 μM. Both the amplitude of the peak at about 150 μM gallamine and the value of $Y_{[G]\rightarrow\infty}$ were unchanged between 9 h and 21 h. Gallamine therefore stabilized the receptor when present at concentrations sufficient to occupy the sites of intermediate affinity ($K_2 \approx 71$ μM), and under those conditions the system appeared to attain equilibrium within 9 h.

Values of F_2 and F_3 tended to be correlated in analyses such as those depicted in Figures 2 and 3, leading to a shallow minimum in the sum of squares with respect to either parameter. The minimum was confirmed by mapping the sum of squares with respect to the value of F_3, which then was fixed accordingly in subsequent analyses. With receptor from *Sf*9 cells, the value of 1 obtained after incubation for 21 h at 30 °C suggests that the intrinsic maximum was equal to the level of binding in the absence of gallamine (Table 3, Figure S10). With receptor from porcine atria, a value of 4 was obtained after incubation for 15 h at 30°C (Table 3): that is, prior to the onset of instability but after the attainment of equilibrium. Since F_3 exceeded 1, intermediate concentrations of gallamine were capable in principle of inducing a level of binding greater than that attained in its absence (*i.e.*, a net increase in binding). A small overshoot was observed experimentally after incubation for 21 h at 37 °C (Figure 2E).

Serpentine effects point to at least three sites for gallamine. For binding at 30 or 37 °C, the values of both $n_{H(1)}$ and $n_{H(3)}$ can be fixed at 1 without an appreciable increase in the sum of squares over that from the fits represented in Table 3 ($P > 0.05$); accordingly, a single site can account for the effect of gallamine in each case. In contrast, the value of $n_{H(2)}$ significantly exceeded 1 under all conditions ($P < 0.001$), suggesting the involvement of at least two sites. It follows that at least four sites are required to account for the data represented in Figures 2 and 3.

The binding of gallamine was compared at different concentrations of *N*-[^{3}H]methylscopolamine in extracts from *Sf*9 cells at 30°C (Figure 4). The samples were incubated for 21 h, which was sufficient for the attainment of equilibrium, and occupancy by the radioligand in the absence of gallamine ranged from 12% at 1.6 nM *N*-[^{3}H]methylscopolamine to 94% at 200 nM (Table 4). Assays in which samples were incubated in parallel for 3 h and 21 h confirmed that the receptor was stable at each level of occupancy for the duration of the assay. A serpentine pattern was obtained at all concentrations of the radioligand except 200 nM (Figure 4).

Data acquired at concentrations of *N*-[^{3}H]methylscopolamine from 1.55 nM to 112 nM were analyzed simultaneously in the manner described above. There was no appreciable increase in the sum of squares with single values of $n_{H(j)}$ for all of the data rather than with separate values for the data at each concentration of the radioligand ($P = 0.42$). There also was no appreciable increase when the common values of both $n_{H(1)}$ and $n_{H(3)}$ were fixed at 1 rather than optimized ($P = 0.09$). In contrast, the value of $n_{H(2)}$ was found to be significantly greater than 1 ($P < 0.00001$) but indistinguishable from 2 ($P = 0.46$). At least four gallamine-

specific sites therefore appear to be involved at all concentrations of *N*-[^{3}H]methylscopolamine.

Increased occupancy by *N*-[^{3}H]methylscopolamine was accompanied by a decrease in the relative amount of binding affected by gallamine via the allosteric sites corresponding to K_1 and K_2, as indicated by the decrease in F_1 and F_2 (Table 4). The effect is illustrated in Figure 4C, where selected curves from panels *A* and *B* have been normalized to the level of binding in the absence of gallamine taken as 100. The concentration of *N*-[^{3}H]methylscopolamine had no appreciable effect on the values of K_j (Table 4), as illustrated in Figure 4D. A different pattern emerged at the highest concentration of *N*-[^{3}H]methylscopolamine, where the binding profile is triphasic downward. The values of K_1 and K_2 are in agreement with those at lower concentrations of the ligand, whereas that of K_3 is about 40-fold higher (Table 4, Figure 4D).

Equilibration of N-[^{3}H]Methylscopolamine and Gallamine with Membrane-bound M_2 Receptor

Receptor in membranes from porcine sarcolemma and transfected CHO cells resembled that in solubilized preparations (Figure 5). The effect of gallamine after incubation for 3 h at 24 °C was biphasic downward, and the fraction of sites exhibiting low affinity increased with the concentration of *N*-[^{3}H]methylscopolamine (Figure 5, panels A and D). Incubation for 48 h (porcine atria) or 16 h (CHO cells) resulted in a peak at 200 μM gallamine, the amplitude of which increased with the concentration of *N*-[^{3}H]methylscopolamine (Figure 5, panels B and E). Essentially the same pattern was obtained after incubation for 5 days (Figure 5C) or 48 h (Figure 5F). The lines in Figure 5 represent best fits of Equation 3, and the parametric values are listed in Table S7.

Prolonged incubation led to a loss of binding at low concentrations of gallamine, as seen in the decrease in $Y_{[G]\rightarrow 0}$ over time (Figures 5A and 5D, insets). The loss was slowed by *N*-[^{3}H]methylscopolamine and prevented by the further inclusion of gallamine at concentrations above 10 μM. Both the magnitude of the effect and the rate were greater with atrial membranes than with membranes from CHO cells. The amplitude of the peak at 200 μM gallamine was established within 48 h (porcine atria) or 16 h (CHO cells) and remained unchanged thereafter. The system therefore appeared to attain equilibrium with respect to binding of the ligands, and gallamine prevented a loss of sites that otherwise occurred in its absence.

The value of K_1 tended to increase with the concentration of the radioligand (Table S7, Figure S12), but the changes were smaller than expected for competition with *N*-[^{3}H]methylscopolamine at the orthosteric site (Figure S12). The values of $n_{H(2)}$ and $n_{H(3)}$ were indistinguishable from 1 throughout and were fixed accordingly; in contrast, the value of $n_{H(1)}$ was near 1 after 3 h but significantly greater at longer times (Table S7). Higher values of $n_{H(1)}$ tended to accompany the loss of sites that occurred in the absence of gallamine, suggesting that they arose in part as an artifact of the protection afforded by the allosteric ligand. In the case of CHO membranes, however, higher values of $n_{H(1)}$ occurred when there was little or no loss of sites: for example, a value of 2.41 was observed after 16 h at 3 nM *N*-[^{3}H]methylscopolamine (Figure 5E, Table S7). At least two sites therefore appear to underlie the interaction identified as K_1.

Cholesterol has been identified as a determinant of homotropic cooperativity among orthosteric sites within oligomers of the M_2 receptor (35). To probe for an effect on the allosteric interaction between gallamine and *N*-[^{3}H]methylscopolamine, the level in sarcolemmal membranes was reduced 25-fold, from 2.3 to 0.093 g of cholesterol per g of total protein. Binding to cholesterol-depleted membranes resembled binding to native

membranes (Figure S13), as did the fitted parametric values from Equation 3 (Table S8). The effect of gallamine was biphasic downward after 3 h at 24°C and serpentine after 48 h. Also, the fractional contribution of the low-affinity component measured at 3 h and the amplitude of the emergent peak measured after 48 h increased with the concentration of the radioligand (Figure S13). Cholesterol therefore does not appear to affect the binding of gallamine or its effect on that of *N*-[^{3}H]methylscopolamine to membrane-bound receptor.

The serpentine pattern observed in buffer B also was observed at higher ionic strength in Dulbecco's phosphate-buffered saline containing calcium and magnesium (Figure S14). Receptor in membranes from CHO cells displayed a small peak at 0.5–2 mM gallamine after incubation for 3 h at 24 °C, and the amplitude increased over time to level off by 48 h. The Hill coefficient was near 1 at each class of sites, and the values of log K_j were similar or somewhat larger than those obtained in buffer B (Table S9). It follows that the serpentine effect common to all preparations in buffer B is not a consequence of low ionic strength or the absence of divalent metal ions.

Pre-mixing of Solubilized Receptor with N-[^{3}H]Methylscopolamine or Gallamine

When receptor extracted from porcine atria was premixed with gallamine, a serpentine pattern developed within 6 h of the addition of *N*-[^{3}H]methylscopolamine and remained essentially the same after 15 h; incubation for 21 h resulted in a loss of binding at low concentrations of gallamine with no change in the amplitude of the peak at 100 μM gallamine (Figure 6). The overall pattern therefore was independent of the order of mixing, but equilibration was more rapid when the allosteric ligand preceded *N*-[^{3}H]methylscopolamine (cf. Figure 2 and Figure 6). Whereas binding became independent of time within 6 h of adding the radioligand to premixed samples (Figure 6), at least 15 h were required after simultaneous addition (Figure 2). A similar result was obtained with receptor extracted from *Sf*9 cells (Figure S15, Table S10).

Premixing the atrial receptor with *N*-[^{3}H]methylscopolamine led initially to a U-shaped binding profile that lacked the third, descending limb of the patterns obtained under other conditions (Figure 6A–C). Incubation for 21 h resulted in a small inhibitory effect at the highest concentration of gallamine, and the resulting serpentine-like pattern became more pronounced after 30h (Figures 6D and 6E). The protection afforded by gallamine at shorter times was lost or diminished after about 21 h, and incubation for 30 h saw a marked loss of binding at all concentrations of the allosteric ligand (Figure 6E). The eventual appearance of a third inflection in samples premixed with *N*-[^{3}H]methylscopolamine suggests that the pattern was tending toward that obtained after simultaneous addition or premixing with gallamine. Convergence could not be observed, however, owing to the loss of receptor upon prolonged incubation.

The estimates of K_1 and K_2 for gallamine were largely unaffected by the order of mixing in extracts from atria or *Sf*9 cells, although they varied over time in both preparations (Figure 6F, Table 5; Figure S15C, Table S10). The value of K_3 was undefined for the atrial receptor premixed with *N*-[^{3}H]methylscopolamine, but the values were similar after premixing with gallamine and after the simultaneous addition of both ligands (Figure 6F). The similarities in K_1 and K_2 suggest that the two limbs of the U-shaped profiles obtained upon preincubation with *N*-[^{3}H]methylscopolamine arose from the same underlying interactions as the corresponding inflections of the serpentine curves obtained under other conditions. Similar agreement also was found among the estimates of $n_{H(j)}$, which were near or equal to 1 for the sites of highest and lowest affinity (*i.e.,* $n_{H(1)}$ and $n_{H(3)}$) (Table 5, Table S10). The value of $n_{H(2)}$ was near 1 in the case of atrial receptor premixed with gallamine (Table 5) and otherwise exceeded 1 (Table 5, Table S10). The order of mixing was without effect on the stability of the receptor from porcine atria (Figure 6).

Pre-mixing of Membrane-bound Receptor with N-[^{3}H]Methylscopolamine

Simultaneous addition of gallamine and *N*-[^{3}H]methylscopolamine to receptor in *Sf*9 membranes led to a serpentine profile with a peak at 0.1–0.5 mM gallamine (Figures 7A and 7B). The peak matured within 48 h and remained unchanged for at least 5 days, while binding at low concentrations of gallamine decreased by 60% over the same period (Figure 7B, inset). The ligands therefore appeared to equilibrate with the receptor within 48 h, and a time-dependent loss of sites was prevented by gallamine. Premixing with *N*-[^{3}H]methylscopolamine led to a U-shaped pattern, and the asymptotic levels of binding at low and high concentrations of gallamine decreased over time. Similar results were obtained with receptor from porcine atria, although the peak that developed at 0.2–0.6 mM gallamine was small (Figures 7D and 7E).

At lower concentrations of gallamine (< 10 μM), binding of *N*-[^{3}H]methylscopolamine decreased at about the same rate irrespective of the order of mixing in either preparation (Figure 7). At higher concentrations (> 10 μM), binding decreased over time when *N*-[^{3}H]methylscopolamine preceded gallamine and increased when the two ligands were added together. The two binding profiles therefore appeared to converge. After incubation for 5 days, the level of binding at or below 0.3 mM gallamine was similar or the same irrespective of the order of mixing (Figures 7B and 7E). It follows that the decrease in binding at higher concentrations of gallamine in samples premixed with *N*-[^{3}H]methylscopolamine was not due to a loss of receptor; rather, it appeared to derive from a process that was rate-limited by the dissociation of *N*-[^{3}H]methylscopolamine in the presence of the allosteric ligand. Samples preincubated with the radioligand therefore were approaching a state of equilibrium that was attained within 48 h when the two ligands were added together.

The order of mixing also was without effect on the estimated values of K_1 and K_2, which increased as the time of incubation was extended from 3 to 48 h (Table S11). There was no further change after incubation for 5 days, suggesting that the underlying interactions were at equilibrium within 48 h. Similarities in the estimates of K_1 and K_2 suggest that the U-shaped patterns observed after premixing with *N*-[^{3}H]methylscopolamine are a kinetic effect: that is, the descending limb corresponding to K_3 was not observed owing to the failure of the radioligand to dissociate on the time-scale of the assay.

Most Hill coefficients were not well defined by the data and therefore were constrained during the analyses. Such constraints were without appreciable effect on the sum of squares ($P > 0.05$) or the values of other parameters. Following the simultaneous addition of *N*-[^{3}H]methylscopolamine and gallamine, the values of $n_{H(2)}$ and $n_{H(3)}$ for receptor in *Sf*9 membranes were fixed at those obtained after extraction in digitonin–cholate (cf. Tables 3 and S11). The corresponding values for receptor in atrial membranes were fixed at 1 (Table S11). Prolonged incubation of either preparation led to an increase in the value of $n_{H(1)}$ from near 1 to 3–4, at least partly as a consequence of instability and the protection afforded by gallamine. When the receptor was premixed with *N*-[^{3}H]methylscopolamine, the values of $n_{H(1)}$ and $n_{H(2)}$ tended to exceed 1 in both preparations.

Equilibration of [^{3}H]Quinuclidinylbenzilate and Gallamine with Solubilized M_2 Receptor

The binding of [^{3}H]quinuclidinylbenzilate to receptor extracted from *Sf*9 membranes was inhibited by gallamine in a biphasic manner (Figure 8). The measurements were taken after incubation of the reaction mixture for different times at two concentrations of [^{3}H]quinuclidinylbenzilate (*i.e.*, 3.9 nM and 22 nM), and the data were analyzed in terms of Equation 3 ($n = 2$) to obtain the lines shown in Figure 8 and the parametric values listed in Table 6. At each concentration of the radioligand, an increase in the time of incubation from 6 h to 30 h was accompanied by a decrease in the value of K_1 and an increase in that of K_2.

There was no further change after incubation for 40 h, suggesting that 30 h was sufficient for the attainment of equilibrium. The fitted value of F_2 was independent of time at either concentration of [^{3}H]quinuclidinylbenzilate, and the values of $n_{H(j)}$ were indistinguishable from 1 throughout ($P > 0.05$).

A 5.8-fold increase in the concentration of [^{3}H]quinuclidinylbenzilate decreased the value of K_1 at equilibrium by 2.5-fold, an effect that cannot be competitive. Similarly, the twofold increase in K_2 at the sites of lower affinity is disproportionately small for a competitive effect, which would be expected to yield a 3.5-fold increase on the basis of the affinity of the radioligand (*i.e.,* K_P = 3.4 nM, Table S1). At each concentration of [^{3}H]quinuclidinylbenzilate, the value of F_2 agreed closely with the percentage occupancy of the receptor by the radioligand in the absence of gallamine (*i.e.*, 0.59 and 54% occupancy at 3.9 nM, 0.85 and 87% occupancy at 22 nM). The receptor was stable for up to 40 h at the higher concentration of [^{3}H]quinuclidinylbenzilate, whereas incubation beyond 12 h resulted in a 13% loss of sites at the lower concentration.

DISCUSSION

Multiple Allosteric Sites

Gallamine has revealed a striking heterogeneity in its allosteric effects at the M_2 muscarinic receptor. Four sites appear to be involved. The rate at which [^{3}H]quinuclidinylbenzilate dissociated from the orthosteric site was modulated in a bell-shaped manner, revealing at least two classes of allosteric sites, and Hill coefficients greater than 1 point to at least three classes overall. In assays at or approaching equilibrium, the binding of [^{3}H]quinuclidinylbenzilate was decreased in a biphasic manner that also indicates two or more classes of allosteric sites. The corresponding effect on the binding of *N*-[^{3}H]methylscopolamine was triphasic and serpentine, which points to at least three classes of sites, and a fourth class is suggested by Hill coefficients greater than 1. Essentially the same pattern was obtained irrespective of temperature and in five preparations of receptor: extracts from porcine atria (4 °C, 30 °C, and 37 °C), extracts from baculovirus-infected *Sf*9 cells (30 °C), and homogenates of porcine atria, *Sf*9 cells, and CHO cells (24 °C).

The existence of two or more allosteric sites also can be inferred from variations in the time required for binding to attain equilibrium, which depended upon the sequence in which gallamine and *N*-[^{3}H]methylscopolamine were added to the receptor. The order of mixing determines the initial conditions for subsequent equilibration of the system. In the case of a monomeric receptor with one allosteric and one orthosteric site, shown in Scheme 2, those conditions are defined by the levels of ligand-free receptor (R), the gallamine-receptor complex (AR), and the radioligand-receptor complex (RL).

To examine the determinants of equilibration in Scheme 2, the time-course for each species of receptor was computed for mixtures of different initial composition. The rate constants used in the simulations are typical of those measured for gallamine and *N*-[^{3}H]methylscopolamine at the M_2 receptor (Table S12). With the model taken as shown, total bound radioligand (*i.e.*, RL plus ARL) was found to equilibrate at a rate that is the same irrespective of the initial conditions and hence of the order of mixing (Figure S16). With a variant in which formation and dissociation of the ternary complex occurs exclusively via RL (*i.e.,* $k^+_{LA} = 0$ and $k^-_{LA} = 0$), the rate of equilibration is sensitive to the initial conditions in a manner that depends upon the concentration of the allosteric ligand. At lower concentrations of A, the prior addition of either ligand causes equilibration to be slower than when both are added together (Figure S17, Table S13); at higher concentrations of A, equilibration is hastened by the prior addition of L and slowed by the prior addition of A (Table S13). Such a restricted model has been found to describe the interaction between

N-[^{3}H]methylscopolamine and alcuronium at the M_2 receptor, where association and dissociation of the former were blocked by the latter (50).

The simulations demonstrate that Scheme 2 cannot account for the present results. Equilibration with the M_2 receptor was fastest when gallamine preceded *N*-[^{3}H]methylscopolamine, somewhat slower when both ligands were added together, and much slower when *N*-[^{3}H]methylscopolamine preceded gallamine. In contrast, the system in Scheme 2 attains equilibrium at a rate that is independent of the initial conditions when the ternary complex is accessible via AR and RL. When access via AR is denied, the differences predicted by the model are at variance with those observed experimentally. The failure of Scheme 2 implies a need for additional reaction pathways and therefore additional sites.

Several lines of evidence indicate that the heterogeneity detected by gallamine is evident at thermodynamic equilibrium. In extracts from *Sf*9 cells, the biphasic inhibitory effect on the binding of [^{3}H]quinuclidinylbenzilate at 30 °C was visible after incubation of the reaction mixture for 6 h and became independent of time after 30 h. Similarly, the serpentine effect on the binding of *N*-[^{3}H]methylscopolamine emerged over time and stabilized after a period that depended upon the preparation and the conditions of the assay. Extracts from porcine atria and CHO cells underwent a time-dependent loss of sites at low concentrations of gallamine, which precluded the attainment of equilibrium under those conditions. There was no loss at higher concentrations, however, and the process of equilibration could be monitored until the amplitude of the peak at about 0.1 mM gallamine became independent of time. The serpentine effect also was independent of the order in which gallamine and *N*-[^{3}H]methylscopolamine were mixed with the receptor. The pattern obtained when gallamine preceded *N*-[^{3}H]methylscopolamine was virtually identical to that when the two ligands were added together, while pretreatment with the radioligand led initially to a U-shaped pattern that became serpentine in nature over time.

All effects of gallamine were allosteric. With *N*-[^{3}H]methylscopolamine, the first descending limb of the serpentine binding profile ($-\log K_1$ = 6.8–6.2, Table 3) occurred at concentrations similar to those that effected the decrease in the rate of dissociation ($\log K_1$ = −5.95, Table 1). The latter interaction is clearly allosteric, and the similarity suggests that the same sites mediate both effects. Comparable agreement is seen with [^{3}H]quinuclidinylbenzilate, where the potencies measured for the biphasic inhibitory effect of gallamine at equilibrium ($\log K_1 \approx -6.1$, $\log K_2 \approx -3.7$, Table 6) recall those inferred from its bell-shaped effect on the rate of dissociation ($\log K_1 \approx -6.0$, $\log K_2 \approx -4.3$). In assays at equilibrium, the noncompetitive nature of the effect at each class of sites is confirmed by the disproportionately small or negligible change in the apparent affinity of gallamine as the concentration of *N*-[^{3}H]methylscopolamine or [^{3}H]quinuclidinylbenzilate was varied over a range that bracketed its equilibrium dissociation constant (*i.e.*, $0.14K_D$–$19K_D$ and $1.5K_D$–$8.9K_D$, respectively). Finally, binding of either radioligand at saturating concentrations of gallamine exceeded nonspecific binding as defined by a saturating concentration of atropine, indicating the formation of a complex that comprises all three of receptor, gallamine, and the radioligand.

The heterogeneity described here has been largely absent from previous reports, in which gallamine generally has been found to interact with a single allosteric site (*e.g.*, (30)). The discrepancy can be attributed variously to the choice of radioligand, the nature of the preparation, the range of concentration used to define the binding profile, and a failure to attain thermodynamic equilibrium.

In most investigations, the orthosteric radioligand has been *N*-[^{3}H]methylscopolamine. Its rate of dissociation is decreased by gallamine in a monophasic manner with a Hill

coefficient near 1 (Figure 1), and one allosteric site therefore has been sufficient to account for the data (*e.g.*, (51)). Studies on the dose-dependence of binding *per se* typically have been performed on membrane-bound receptors at low levels of occupancy by the radioligand and after comparatively short periods of incubation. Such conditions reveal only the sites of highest affinity for gallamine (K_1), and the serpentine nature of the binding pattern is obscured. The sites of intermediate and lowest affinity (K_2 and K_3) require prolonged incubation and higher levels of occupancy, exceeding 50% of the orthosteric sites in the case of atrial and CHO membranes (Figure 5). When the level of occupancy by *N*-[^{3}H]methylscopolamine has exceeded 50%, however, the time of incubation has been less than 9 h (52;53); when the time of incubation has exceeded 18 h, the level of occupancy has been less than 50% (54;55). Also, the highest concentration of gallamine rarely has exceeded 10 μM, which encompasses K_1 but is about tenfold less than K_2. The serpentine pattern can be detected more readily where it emerges sooner and at lower concentrations of *N*-[^{3}H]methylscopolamine, as in the case of solubilized extracts, *Sf*9 membranes, and possibly membranes from N1E-115 neuroblastoma cells (56).

It has been noted previously that the effect of an allosteric ligand can depend upon the choice of orthosteric probe (*e.g.*, (53;57)). This is consistent with the reciprocal nature of heterotropic interactions, and it is illustrated here by differences in the binding patterns obtained with *N*-[^{3}H]methylscopolamine and [^{3}H]quinuclidinylbenzilate as the system approached equilibrium. An interdependence between the orthosteric and allosteric ligand also is observed in the rate of dissociation at different concentrations of [^{3}H]quinuclidinylbenzilate, which differed only in the presence of gallamine (Figure 1D). By this measure, the affinity of [^{3}H]quinuclidinylbenzilate was reduced 14-fold, from 0.022 nM for the vacant receptor (Table S1) to 0.31 nM at saturating concentrations of gallamine (Figure S9).

Origin of Heterogeneity

Muscarinic receptors were exclusively or predominantly of the M_2 subtype in all preparations, including those from porcine atria (58). It follows that the heterogeneity revealed in the binding of gallamine was induced in an otherwise homogeneous population of sites. G proteins can induce multiple states of affinity for agonists at M_2 muscarinic and other G protein-coupled receptors (8;59;60), but they appear not to be implicated in those reported here for gallamine. Preparations from porcine atria and *Sf*9 cells gave essentially the same results, and there is little or no effect of endogenous G proteins on the binding properties of GPCRs expressed in *Sf*9 cells (61;62). Also, the bell-shaped effect of gallamine on the dissociation of [^{3}H]quinuclidinylbenzilate has been described previously for M_2 receptors in CHO membranes, where it was not affected by treatment with pertussis toxin (32).

Heterogeneity independent of a G protein or other third party could arise from interactions among receptors within an oligomer. With one allosteric site per protomer, the four sites recognized by gallamine point to an array that is tetrameric or larger. Such an oligomer may be intrinsically asymmetric, with protomers having different affinities in the absence of any ligand, but that alone seems insufficient. Gallamine differed in its effects on the binding of *N*-[^{3}H]methylscopolamine and [^{3}H]quinuclidinylbenzilate, and the pattern varied with the concentration of the radioligand in each case. These observations suggest that the observed heterogeneity derives in part from differences in the magnitude of heterotropic cooperativity between different pairs of protomers. Pre-existing or intrinsic asymmetry also cannot account for Hill coefficients greater than 1, which imply a degree of positive homotropic cooperativity between successive equivalents of gallamine. It follows that multiple values of K_j may arise from a blend of asymmetry, homotropic cooperativity in the binding of gallamine, and heterotropic cooperativity between gallamine and the radioligand.

All interactions between orthosteric and allosteric sites appear to occur within an oligomer of the same size under all conditions. The bell-shaped effect of gallamine on the rate of dissociation of [^{3}H]quinuclidinylbenzilate and the serpentine effect on the binding of *N*-[^{3}H]methylscopolamine were broadly similar with receptor from different sources, both in membranes and in solubilized preparations. With the membrane-bound receptor, the effect on the dissociation of [^{3}H]quinuclidinylbenzilate was essentially insensitive to the level of cholesterol, treatment with DTT, or small differences in ionic strength; similarly, the effect on the binding of *N*-[^{3}H]methylscopolamine was insensitive to ionic strength or the level of cholesterol. The conservation of such effects under disparate conditions suggests that they are native to the receptor and not an artefactual consequence of any particular treatment or set of conditions. The inherent nature of M_2 receptors to form oligomers has been demonstrated by the spontaneous formation of tetramers when purified monomers are reconstituted into phospholipid vesicles (22). The ability of oligomers to survive extraction has been demonstrated by co-immunoprecipitation and cross-linking of receptors solubilized from native membranes and in reconstituted preparations (18;22).

There appear to have been few if any monomers, at least with receptor extracted from *Sf*9 membranes. In that case, the dissociation of *N*-[^{3}H]methylscopolamine in the absence of gallamine was monoexponential with a rate constant of 0.06 ± 0.001 min $^{-1}$. There was no evidence for a slower process with a rate constant of 0.036 ± 0.001 min $^{-1}$, which is the value reported for the dissociation of *N*-[^{3}H]methylscopolamine from monomers of the M_2 receptor purified from *Sf*9 membranes (42). The apparent absence of monomers is consistent with the observation that M_2 receptors extracted from *Sf*9 membranes in cholate–NaCl migrated exclusively as oligomers following treatment with the cross-linking reagent BS^3 (35).

An allosteric site on each of four linked protomers is consistent with pharmacological, biochemical, and biophysical evidence that M_2 receptors exist predominantly or exclusively as tetramers, both in membranes and in solubilized extracts from various sources. The guanylyl nucleotide-sensitive heterogeneity revealed by agonists at the orthosteric site of cardiac muscarinic receptors can be described quantitatively in terms of cooperative interactions within an array that is tetrameric or larger (19). Essentially the same properties are recovered when purified monomers of the M_2 receptor are reassembled as tetramers in phospholipid vesicles (22). Muscarinic receptors purified from porcine atria have been found to migrate in part with the electrophoretic mobility expected of a tetramer (28), and three differently tagged M_2 receptors have been copurified from triply infected *Sf*9 cells in quantities sufficient to suggest that the complex is larger than a trimer (18). Finally, a model-based analysis of FRET efficiencies between eGFP and eYFP has suggested that fluorophore-tagged M_2 receptors exist primarily as tetramers when coexpressed in CHO cells (24).

Nature of Heterogeneity within a Tetramer

Two observations offer some insight into how biphasic and serpentine binding profiles might emerge from linked sites within a tetramer. First, higher levels of occupancy by [^{3}H]quinuclidinylbenzilate or *N*-[^{3}H]methylscopolamine were accompanied by a decrease in the apparent fraction of labeled sites exhibiting the highest affinity for gallamine (*i.e.,* K_1 in Equation 3) and a concomitant increase in the fraction or fractions exhibiting lower affinity (*i.e.,* K_2 and K_3). Second, monomers of the M_2 receptor purified from *Sf*9 cells have been shown to bind gallamine with an affinity of 75 μM (log K = −4.12), as inferred from its effect on the rate of dissociation of *N*-[^{3}H]methylscopolamine (42). That value exceeds the present values of K_1 from similar experiments by at least 60-fold (Table 1). It also exceeds the present value of K_1 from the serpentine effect by 50-fold and the value of K_2 by about

threefold (Table 3), suggesting that K_3 arises from heterotropic cooperativity between sites on the same protomer.

A model that rationalizes these observations in the context of cooperativity within a tetramer is illustrated in Figure 9. The apparent affinity of a ligand for the allosteric site on one protomer is determined by the overall liganded status and configuration of the complex. It is highest when the orthosteric sites of the same and neighboring protomers are vacant, and it is weakest when the orthosteric site of the same protomer is occupied. The heterogeneity derives from a combination of heterotropic cooperativity between allosteric and orthosteric sites and homotropic cooperativity at either or both. At the level of a pairwise interaction, net heterotropic cooperativity depends upon whether the participating sites are located on the same or different protomers and whether the latter are immediate neighbors or more distant.

In the case of *N*-[^{3}H]methylscopolamine, binding of the radioligand to one of the four orthosteric sites creates at least three classes of allosteric sites and three modes of heterotropic cooperativity. The highest apparent affinity for gallamine (K_1) derives from protomers diagonally opposite the labeled protomer, and intermolecular negative cooperativity accounts for the first, downward inflection in the serpentine binding profile. The intermediate affinity (K_2) derives from protomers adjacent to the labeled protomer, and intermolecular positive cooperativity or attenuated negative cooperativity accounts for the upward transition. Allosteric sites on labeled protomers are of weakest affinity, and intramolecular negative cooperativity accounts for the final descending limb of the binding profile (K_3).

The model depicted in Figure 9 suggests an explanation for the progressive decrease in F_1 as the concentration of *N*-[^{3}H]methylscopolamine was increased from 1.6 to 112 nM (Figure 4, Table 4). Higher concentrations of the radioligand would decrease the prevalence of allosteric sites on vacant protomers, thereby decreasing the likelihood of intermolecular heterotropic cooperativity (F_1) and increasing that of intramolecular heterotropic cooperativity (F_3). As occupancy by the radioligand approached saturation (*i.e.*, 94.3% at 200 nM), however, the serpentine nature of the effect was lost. Gallamine became strictly inhibitory, albeit in a triphasic manner, and 76% of the decrease in binding was associated with the sites of intermediate affinity (F_2). Although such an effect is further evidence for the cooperative nature of events within the oligomer, an understanding how it arises is likely to require an explicit mechanistic description of the system.

At least one inflection of the serpentine profile displayed by gallamine was characterized by a Hill coefficient greater than 1, which has implications for the organization of the structure in Figure 9. In the case of solubilized preparations at 30 °C, the value of 1.5–1.8 obtained for $n_{H(2)}$ points to positive homotropic cooperativity between the allosteric sites of two protomers adjacent to the single protomer bearing a radioligand (Table 3). In the case of homogenates, the high values of $n_{H(1)}$ suggest that positive cooperativity occurs between a site opposite the labeled protomer and an adjacent site (Table S7). Such a shift in the cooperative effect from the first and second equivalents of gallamine (K_1) to the second and third equivalents (K_2) implies that the tetramer does not function as a dimer of dimers.

In the case of [^{3}H]quinuclidinylbenzilate, the biphasic nature of the binding profile suggests that the affinity of gallamine for an allosteric site is largely independent of its location on a protomer adjacent to or diagonally opposite a labeled protomer; rather, the relationship between the value of F_2 defined by gallamine and the fraction of sites occupied by [^{3}H]quinuclidinylbenzilate suggests that the affinity for the allosteric ligand is determined simply by the absence or the presence of the radioligand. Protomers with a vacant

orthosteric site are of higher affinity for gallamine, and those in which the orthosteric site is occupied by the radioligand are of lower affinity.

To examine the plausibility of a model such as that in Figure 9, the effects of interactions between allosteric and orthosteric ligands were simulated in terms of Scheme 3. The species shown as R has two allosteric and two orthosteric sites and therefore can be taken to represent a dimer, each protomer of which has one site for each ligand. A dimer is simpler than the tetramer required by the present data, but it also is more tractable. Whereas the mathematical representation of Scheme 3 comprises 16 differential equations and 64 first- and second-order rate constants, the corresponding description of a tetramer comprises 256 differential equations and 2,048 rate constants. It is of interest to note that Scheme 3 also could be taken to represent the four orthosteric sites of a heterotetramer comprising two protomers of one GPCR and two of another.

The distribution of receptors among the 16 different species of Scheme 3 was simulated with respect to the concentration of the allosteric ligand (A) at different times and at different concentrations of the orthosteric probe (L). The rate constants were set to yield effects that resemble those obtained experimentally with gallamine and *N*-[^{3}H]methylscopolamine at the M_2 receptor. Ligand A was assumed to slow both the association and the dissociation of ligand L, but in a disproportionate manner that was achieved by partitioning the cooperativity factor (α) between the two rate constants. Heterotropic cooperativity between L and A was the sole determinant of heterogeneity revealed by ligand A, which otherwise bound to all allosteric sites with the same affinity. Further details regarding the simulations are described in the supporting information (Figure S2, Table S14).

Defined in this manner, Scheme 3 yields the bell-shaped pattern illustrated in Figure 10. An increase in the time of the reaction is accompanied by an increase in the amplitude of the peak at intermediate concentrations of ligand A (*i.e.*, 1–10 nM), in the asymptotic level of binding at saturating concentrations of A, and in the values of K_1 and K_2 (Figure 10A, Table S15). The Hill coefficient for either inflection is near or equal to 1 throughout (Table S15). With the system at equilibrium, an increase in occupancy at the orthosteric site is accompanied by a decrease in the relative amplitude of the peak at intermediate concentrations of ligand A and an increase in the asymptotic level of binding at saturating concentrations (Figure 10B, Table S15). A threefold increase in the concentration of L, from 0.32 μM to 1.0 μM, is accompanied by a 1.7-fold decrease in the value of K_1 and a comparatively small, 2.3-fold increase in that of K_2 (Table S15).

The results in Figure 10 indicate that Scheme 3 can mimic the effects of gallamine on *N*-[^{3}H]methylscopolamine, confirming that the model presented in Figure 9 is plausible. The bell-shaped profile obtained by simulation is analogous to the peak in the serpentine binding profile, and both were affected in a similar manner by variations in the time of incubation and the level of occupancy by the radioligand. In preparations of the M_2 receptor, the amplitude of the peak increased over time (*e.g.*, Figures 3 and 5) and varied with occupancy (*e.g.*, Figures 4 and 5); at times approaching equilibrium, the potencies corresponding to the rising and descending limbs were essentially independent of the radioligand (*e.g.*, Figure 4D, Table 4) or were affected in a noncompetitive manner (Figure S12, Table S7). The Hill coefficient of 1 obtained for simulated data irrespective of time suggests that the higher values found experimentally were not a kinetic artifact but rather arose from cooperative interactions.

The simulations presented in Figure 10 illustrate how the peak in the serpentine effect of gallamine might arise from heterotropic cooperativity between the allosteric and orthosteric ligands. In the case of Scheme 3, the increase in bound L at lower concentrations of A

derives from positive intermolecular cooperativity between A and L (*i.e.*, $\alpha_{OL}^{AO} \equiv \alpha_{LO}^{OA}=0.0032$); the decrease in bound L at higher concentrations of A derives from the net negative effect of inter-and intramolecular cooperativity between A and L (*i.e.*, $\alpha_{LO}^{AO}\alpha_{LO}^{OA} \equiv \alpha_{OL}^{OA}\alpha_{OL}^{AO}=3.2$). These changes are tracked on the ordinate in the values of F_1 and F_2 (Table S15), respectively, which are a measure of the distribution of L-bearing dimers among the different states.

The increase in binding occurs at concentrations of A that reflect its affinity for L-free protomers associated with L-bearing protomers (*i.e.*, $\alpha_{OL}^{AO}K_A$ or $\alpha_{LO}^{OA}K_A$); the decrease occurs at concentrations that reflect its affinity for L-bearing protomers (*i.e.*, $\alpha_{LO}^{AO}\alpha_{OO}^{AA}K_A$ or $\alpha_{OL}^{OA}\alpha_{OO}^{AA}K_A$). The rate constant for the dissociation of A from any species of receptor in Scheme 3 is at least 6.5-fold greater than that for the dissociation of L; similarly, the rate constant for the association of A is at least 100-fold greater than that for the association of L. The allosteric ligand therefore equilibrates rapidly with a mixture of L-bearing species that is established slowly over the course of the experiment, and the measured values of K_j provide a snapshot of the heterogeneity existing at the time of the assay.

It seems likely that such a rapid equilibration of gallamine at a high-affinity allosteric site distant from an occupied orthosteric site explains the consistent pattern that has emerged from previous studies. In most cases, myocardial membranes have been incubated with *N*-[^{3}H]methylscopolamine for 3 h or less at comparatively low concentrations of gallamine. When sarcolemmal membranes were incubated for 3 h at 24 °C in the present investigation (Figure 5A), the value of log K_1 for gallamine increased from −7.27 at 0.1 nM *N*-[^{3}H]methylscopolamine to −6.55 at 3 nM (Table S7). If the failure to obtain equilibrium and the measurements above 0.1 mM gallamine are disregarded, the data are well described by Scheme 2 with a cooperativity factor of about 70 (*i.e.*, $1/\alpha$) (Figure S18, Table S16). A similar value of 46 has been reported previously for the allosteric interaction between *N*-[^{3}H]methylscopolamine and gallamine at similarly restricted concentrations of gallamine (63).

Broader Implications of Oligomers for Allosteric Regulation and Signaling

Effects similar to those described here for gallamine have been reported for other modulators and argue similarly for two or more allosteric sites. The effect of KT5720 on the rate of dissociation of *N*-[^{3}H]methylscopolamine was bell-shaped with M_1 receptors in CHO membranes (64), and that of obidoxime was biphasic downward with M_2 receptors in myocardial membranes (65). The allosteric ligands tacrine, Duo-3, KT5823, and Go7874 have been found to inhibit the specific binding of *N*-[^{3}H]methylscopolamine with Hill coefficients greater than 1 at various subtypes of muscarinic receptor (64;66;67). Gallamine has been shown to affect the affinities of agonists for the M_2 receptor without affecting efficacy, implying that at least two orthosteric sites are modulated by the allosteric ligand (48).

Such effects of allosteric modulators typically have been rationalized in terms of two or more sites on a monomer. In the case of the D_2 dopamine receptor and the M_2 muscarinic receptor, it has been suggested that the allosteric ligand binds promiscuously to the orthosteric and allosteric sites in a cooperative manner, thereby giving rise to Hill coefficients greater than 1 in some studies (68-70). It also has been suggested that a monomer of the M_1 receptor contains two topographically distinct allosteric sites in addition to the orthosteric site (64). In both cases, however, an interpretation based on monomers falls short when probed directly using the radiolabelled allosteric ligand [^{3}H]dimethyl-W84 (67). More complex behavior also has been rationalized in terms of kinetically determined

effects in a system not at equilibrium, although the rate constants were not constrained in accord with the expectations of microscopic reversibility (52).

Alcuronium is the prototypic positive allosteric modulator of muscarinic receptors (71), and its bell-shaped effect on the binding of *N*-[^{3}H]methylscopolamine recalls the serpentine effect of gallamine in the present investigation. In contrast, both ligands modulate the binding of [^{3}H]quinuclidinylbenzilate in a strictly inhibitory manner; the effect is monophasic in the case of alcuronium (72) and biphasic in the case of gallamine. The differences suggest that positive heterotropic cooperativity occurs only with *N*-[^{3}H]methylscopolamine, in contrast to the prevailing view that such effects are unique to alcuronium (1). It has been suggested that the distance between the quaternary amino group and the *para*-carbon atom of the phenyl ring in *N*-[^{3}H]methylscopolamine is a determinant of positive heterotropic cooperativity in the interaction with gallamine (57). If heterotropic effects can be intermolecular as well as intramolecular, their direction as positive or negative also is likely to depend upon how the structure of the orthosteric probe affects interactions among the constituent protomers of the oligomer.

Cooperativity within a tetramer can account for apparent heterogeneity and related noncompetitive effects seen in the nucleotide-sensitive binding of agonists (*e.g.*, (26;73)) and in the binding of quinuclidinylbenzilate and *N*-methylscopolamine under some conditions (22;27;35). All such effects involve cooperativity among orthosteric sites, which is necessarily intermolecular in nature. The present results suggest that heterotropic interactions between allosteric and orthosteric sites can be both intra- and intermolecular; they also suggest that neighboring allosteric sites can engage in intermolecular homotropic cooperativity. A picture therefore emerges of a tetrameric receptor with a total of eight orthosteric and allosteric sites, all of which function in a linked manner. Moreover, the serpentine effect of gallamine in the present investigation resembles that reported previously for the allosteric effect of adenylyl nucleotides on the binding of [^{35}S]GTPγS to G proteins linked to muscarinic receptors in myocardial membranes (74). These observations reinforce the notion of a signaling complex comprising multiple copies of receptor and G protein (*e.g.*, (28;75;76)).

Supplementary Material

Refer to Web version on PubMed Central for supplementary material.

Acknowledgments

We are grateful to the managers and staff of Quality Meat Packers Ltd. for generous supplies of porcine atria. We thank Gwendolynne Elmslie for assistance with the binding assays and Drs. Amy Ma and Alejandro Colozo for their help with the processing of atrial tissue.

Funding: This work was supported by grants from the Canadian Institutes of Health Research (MOP-43990, MOP-97978) (to J.W.W.), the Heart and Stroke Foundation of Ontario (T5650, T6280) (to J.W.W.), and the National Institutes of Health (R01AG05214) (to J.E.).

References

1. May LT, Leach K, Sexton PM, Christopoulos A. Allosteric modulation of G protein-coupled receptors. Annu Rev Pharmacol. 2007; 47:1–51.
2. Haga K, Kruse AC, Asada H, Yurugi-Kobayashi T, Shiroishi M, Zhang C, Weis WI, Okada T, Kobilka BK, Haga T, Kobayashi T. Structure of the human M_2 muscarinic acetylcholine receptor bound to an antagonist. Nature. 2012; 482:547–551. [PubMed: 22278061]
3. Huang XP, Prilla S, Mohr K, Ellis J. Critical amino acid residues of the common allosteric site on the M_2 muscarinic acetylcholine receptor: More similarities than differences between the

structurally divergent agents gallamine and bis(ammonio) alkane-type hexamethylene-*bis*-[dimethyl-(3-phthalimidopropyl)ammonium]dibromide. Mol Pharmacol. 2005; 68:769–778. [PubMed: 15937215]

4. Kenakin T. Allosteric modulators: The new generation of receptor antagonist. Mol Interventions. 2004; 4:222–229.
5. Chabre M, le Maire M. Monomeric G-protein-coupled receptor as a functional unit. Biochemistry. 2005; 44:9395–9403. [PubMed: 15996094]
6. Bayburt TH, Leitz AJ, Xie G, Oprian DD, Sligar SG. Transducin activation by nanoscale lipid bilayers containing one and two rhodopsins. J Biol Chem. 2007; 282:14875–14881. [PubMed: 17395586]
7. Kuszak AJ, Pitchiaya S, Anand JP, Mosberg HI, Walter NG, Sunahara RK. Purification and functional reconstitution of monomeric mu-opioid receptors: allosteric modulation of agonist binding by Gi2. J Biol Chem. 2009; 284:26732–26741. [PubMed: 19542234]
8. Whorton MR, Bokoch MP, Rasmussen SGF, Huang B, Zare RN, Kobilka B, Sunahara RK. A monomeric G protein-coupled receptor isolated in a high-density lipoprotein particle efficiently activates its G protein. Proc Natl Acad Sci U S A. 2007; 104:7682–7687. [PubMed: 17452637]
9. Hern JA, Baig AH, Mashanov GI, Birdsall B, Corrie JE, Lazareno S, Molloy JE, Birdsall NJ. Formation and dissociation of M_1 muscarinic receptor dimers seen by total internal reflection fluorescence imaging of single molecules. Proc Natl Acad Sci U S A. 2010; 107:2693–2698. [PubMed: 20133736]
10. Kasai RS, Suzuki KG, Prossnitz ER, Koyama-Honda I, Nakada C, Fujiwara TK, Kusumi A. Full characterization of GPCR monomer-dimer dynamic equilibrium by single molecule imaging. J Cell Biol. 2011; 192:463–480. [PubMed: 21300851]
11. Baneres JL, Parello J. Structure-based analysis of GPCR function: evidence for a novel pentameric assembly between the dimeric leukotriene B4 receptor BLT1 and the G-protein. J Mol Biol. 2003; 329:815–829. [PubMed: 12787680]
12. Han Y, Moreira IS, Urizar E, Weinstein H, Javitch JA. Allosteric communication between protomers of dopamine class A GPCR dimers modulates activation. Nat Chem Biol. 2009; 5:688–695. [PubMed: 19648932]
13. Maurice P, Daulat AM, Turecek R, Ivankova-Susankova K, Zamponi F, Kamal M, Clement N, Guillaume JL, Bettler B, Gales C, Delagrange P, Jockers R. Molecular organization and dynamics of the melatonin MT_1 receptor/RGS20/G_i protein complex reveal asymmetry of receptor dimers for RGS and G_i coupling. EMBO J. 2010; 29:3646–3659. [PubMed: 20859254]
14. Angers S, Salahpour A, Joly E, Hilairet S, Chelsky D, Dennis M, Bouvier M. Detection of β_2-adrenergic receptor dimerization in living cells using bioluminescence resonance energy transfer (BRET). Proc Natl Acad Sci U S A. 2000; 97:3684–3689. [PubMed: 10725388]
15. Overton MC, Blumer KJ. G-protein-coupled receptors function as oligomers in vivo. Curr Biol. 2000; 10:341–344. [PubMed: 10744981]
16. Lopez-Gimenez JF, Canals M, Pediani JD, Milligan G. The α_{1b}-adrenoceptor exists as a higher-order oligomer: effective oligomerization is required for receptor maturation, surface delivery, and function. Mol Pharmacol. 2007; 71:1015–1029. [PubMed: 17220353]
17. Carriba P, Navarro G, Ciruela F, Ferre S, Casado V, Agnati L, Cortes A, Mallol J, Fuxe K, Canela EI, Lluis C, Franco R. Detection of heteromerization of more than two proteins by sequential BRET-FRET. Nat Methods. 2008; 5:727–733. [PubMed: 18587404]
18. Park PS, Wells JW. Oligomeric potential of the M_2 muscarinic cholinergic receptor. J Neurochem. 2004; 90:537–548. [PubMed: 15255931]
19. Chidiac P, Green MA, Pawagi AB, Wells JW. Cardiac muscarinic receptors. Cooperativity as the basis for multiple states of affinity. Biochemistry. 1997; 36:7361–7379. [PubMed: 9200684]
20. Fung JJ, Deupi X, Pardo L, Yao XJ, Velez-Ruiz GA, Devree BT, Sunahara RK, Kobilka BK. Ligand-regulated oligomerization of beta(2)-adrenoceptors in a model lipid bilayer. EMBO J. 2009; 28:3315–3328. [PubMed: 19763081]
21. Guo W, Urizar E, Kralikova M, Mobarec JC, Shi L, Filizola M, Javitch JA. Dopamine D_2 receptors form higher order oligomers at physiological expression levels. EMBO J. 2008; 27:2293–2304. [PubMed: 18668123]

22. Ma AW, Redka DS, Pisterzi LF, Angers S, Wells JW. Recovery of oligomers and cooperativity when monomers of the M_2 muscarinic cholinergic receptor are reconstituted into phospholipid vesicles. Biochemistry. 2007; 46:7907–7927. [PubMed: 17552496]
23. Nimchinsky EA, Hof PR, Janssen WG, Morrison JH, Schmauss C. Expression of dopamine D_3 receptor dimers and tetramers in brain and in transfected cells. J Biol Chem. 1997; 272:29229–29237. [PubMed: 9361002]
24. Pisterzi LF, Jansma DB, Georgiou J, Woodside MJ, Chou JTC, Angers S, Raicu V, Wells JW. Oligomeric size of the M_2 muscarinic receptor in live cells as determined by quantitative fluorescence resonance energy transfer. J Biol Chem. 2010; 285:16723–16738. [PubMed: 20304928]
25. Birdsall, NJ.; Burgen, AS.; Hulme, EC. Correlation between the binding properties and pharmacological responses of muscarinic receptors. In: Jenden, DJ., editor. Cholinergic Mechanisms and Psychopharmacology. Plenum Press; New York: 1977. p. 25-33.
26. Ehlert FJ. The relationship between muscarinic receptor occupancy and adenylate cyclase inhibition in the rabbit myocardium. Mol Pharmacol. 1985; 28:410–421. [PubMed: 4058422]
27. Park PS, Sum CS, Pawagi AB, Wells JW. Cooperativity and oligomeric status of cardiac muscarinic cholinergic receptors. Biochemistry. 2002; 41:5588–5604. [PubMed: 11969420]
28. Wreggett KA, Wells JW. Cooperativity manifest in the binding properties of purified cardiac muscarinic receptors. J Biol Chem. 1995; 270:22488–22499. [PubMed: 7673239]
29. Jensen AA, Spalding TA. Allosteric modulation of G-protein coupled receptors. Eur J Pharm Sci. 2004; 21:407–420. [PubMed: 14998571]
30. Stockton JM, Birdsall NJM, Burgen ASV, Hulme EC. Modification of the binding properties of muscarinic receptors by gallamine. Mol Pharmacol. 1983; 23:551–557. [PubMed: 6865905]
31. Potter LT, Ferrendelli CA, Hanchett HE, Hollifield MA, Lorenzi MV. Tetrahydroaminoacridine and other allosteric antagonists of hippocampal M_1 muscarine receptors. Mol Pharmacol. 1989; 35:652–660. [PubMed: 2725474]
32. Ellis J, Seidenberg M. Gallamine exerts biphasic allosteric effects at muscarinic receptors. Mol Pharmacol. 1989; 35:173–176. [PubMed: 2918854]
33. Conn PJ, Christopoulos A, Lindsley CW. Allosteric modulators of GPCRs: A novel approach for the treatment of CNS disorders. Nat Rev Drug Discov. 2009; 8:41–54. [PubMed: 19116626]
34. Terrillon S, Bouvier M. Roles of G-protein-coupled receptor dimerization - From ontogeny to signalling regulation. EMBO Reports. 2004; 5:30–34. [PubMed: 14710183]
35. Colozo AT, Park PS, Sum CS, Pisterzi LF, Wells JW. Cholesterol as a determinant of cooperativity in the M_2 muscarinic cholinergic receptor. Biochem Pharmacol. 2007; 74:236–255. [PubMed: 17521619]
36. Peterson GL, Herron GS, Yamaki M, Fullerton DS, Schimerlik MI. Purification of the muscarinic acetylcholine receptor from porcine atria. Proc Natl Acad Sci U S A. 1984; 81:4993–4997. [PubMed: 6589642]
37. Peterson GL, Schimerlik MI. Large scale preparation and characterization of membrane-bound and detergent-solubilized muscarinic acetylcholine receptor from pig atria. Prep Biochem. 1984; 14:33–74. [PubMed: 6718325]
38. Ellis J, Huyler J, Brann MR. Allosteric regulation of cloned M_1–M_5 muscarinic receptor subtypes. Biochem Pharmacol. 1991; 42:1927–1932. [PubMed: 1741770]
39. Park P, Sum CS, Hampson DR, Van Tol HH, Wells JW. Nature of the oligomers formed by muscarinic M_2 acetylcholine receptors in *Sf*9 cells. Eur J Pharmacol. 2001; 421:11–22. [PubMed: 11408044]
40. Park PS, Wells JW. Monomers and oligomers of the M_2 muscarinic cholinergic receptor purified from *Sf*9 cells. Biochemistry. 2003; 42:12960–12971. [PubMed: 14596611]
41. Burgmer U, Schulz U, Trankle C, Mohr K. Interaction of Mg^{2+} with the allosteric site of muscarinic M_2 receptors. Naunyn Schmiedebergs Arch Pharmacol. 1998; 357:363–370. [PubMed: 9606020]
42. Redka DS, Pisterzi LF, Wells JW. Binding of orthosteric ligands to the allosteric site of the M_2 muscarinic cholinergic receptor. Mol Pharmacol. 2008; 74:834–843. [PubMed: 18552124]

43. Ellis J, Seidenberg M. Interactions of alcuronium, TMB-8, and other allosteric ligands with muscarinic acetylcholine receptors: studies with chimeric receptors. Mol Pharmacol. 2000; 58:1451–1460. [PubMed: 11093785]
44. Wells, JW. Analysis and interpretation of binding at equilibrium. In: Hulme, EC., editor. Receptor-Ligand Interactions A Practical Approach. Oxford University Press; Oxford: 1992. p. 289-395.
45. Marquardt DW. An algorithm for least-squares estimation of nonlinear parameters. SIAM J Appl Math. 1963; 11:431–441.
46. Kostenis E, Mohr K. Two-point kinetic experiments to quantify allosteric effects on radioligand dissociation. Trends Pharmacol Sci. 1996; 17:280–283. [PubMed: 8810873]
47. Ellis J, Seidenberg M. Competitive and allosteric interactions of 6-chloro-5,10-dihydro-5-[(1-methyl-4-piperidinyl)acetyl]-11H-dibenzo[b,e][1,4]diazepine-11-one hydrochloride (UH-AH 37) at muscarinic receptors, via distinct epitopes. Biochem Pharmacol. 1999; 57:181–186. [PubMed: 9890566]
48. Ehlert FJ, Griffin MT. Two-state models and the analysis of the allosteric effect of gallamine at the M_2 muscarinic receptor. J Pharmacol Exp Ther. 2008; 325:1039–1060. [PubMed: 18305010]
49. Leppik RA, Miller RC, Eck M, Paquet JL. Role of acidic amino-acids in the allosteric modulation by gallamine of antagonist binding at the M_2 muscarinic acetylcholine receptor. Mol Pharmacol. 1994; 45:983–990. [PubMed: 8190113]
50. Proska J, Tucek S. Mechanisms of steric and cooperative actions of alcuronium on cardiac muscarinic acetylcholine receptors. Mol Pharmacol. 1994; 45:709–717. [PubMed: 8183250]
51. Schroter A, Trankle C, Mohr K. Modes of allosteric interactions with free and [^{3}H]N-methylscopolamine-occupied muscarinic M_2 receptors as deduced from buffer-dependent potency shifts. Naunyn Schmiedebergs Arch Pharmacol. 2000; 362:512–519. [PubMed: 11138843]
52. Avlani V, May LT, Sexton PM, Christopoulos A. Application of a kinetic model to the apparently complex behavior of negative and positive allosteric modulators of muscarinic acetylcholine receptors. J Pharmacol Exp Ther. 2004; 308:1062–1072. [PubMed: 14711931]
53. Lee NH, Elfakahany EE. Influence of ligand choice on the apparent binding profile of gallamine to cardiac muscarinic receptors - Identification of 3 main types of gallamine muscarinic receptor interactions. J Pharmacol Exp Ther. 1988; 246:829–838. [PubMed: 3418516]
54. Proska J, Tucek S. Competition between positive and negative allosteric effectors on muscarinic receptors. Mol Pharmacol. 1995; 48:696–702. [PubMed: 7476896]
55. Tucek S, Proska J. Allosteric Modulation of Muscarinic Acetylcholine-Receptors. Trends Pharmacol Sci. 1995; 16:205–212. [PubMed: 7652930]
56. Lee NH, El Fakahany EE. Mixed competitive and allosteric antagonism by gallamine of muscarinic receptor-mediated 2nd messenger responses in N1E-115 neuroblastoma cells. J Neurochem. 1989; 53:1300–1308. [PubMed: 2549200]
57. Lysikova M, Havlas M, Tucek S. Interactions between allosteric modulators and 4-DAMP and other antagonists at muscarinic receptors: Potential significance of the distance between the N and carboxyl C atoms in the molecules of antagonists. Neurochem Res. 2001; 26:383–394. [PubMed: 11495349]
58. Wang HZ, Han H, Zhang LM, Shi H, Schram G, Nattel S, Wang ZG. Expression of multiple subtypes of muscarinic receptors and cellular distribution in the human heart. Mol Pharmacol. 2001; 59:1029–1036. [PubMed: 11306684]
59. Florio VA, Sternweis PC. Reconstitution of resolved muscarinic cholinergic receptors with purified GTP-binding proteins. J Biol Chem. 1985; 260:3477–3483. [PubMed: 3919024]
60. Haga K, Haga T, Ichiyama A. Reconstitution of the muscarinic acetylcholine receptor. Guanine nucleotide-sensitive high affinity binding of agonists to purified muscarinic receptors reconstituted with GTP-binding proteins (Gi and Go). J Biol Chem. 1986; 261:10133–10140. [PubMed: 3015919]
61. Heitz F, Mcclue SJ, Harris BA, Guenet C. Expression of human M_2 muscarinic receptors in *Sf*9 cells - Characterization and reconstitution with G-Proteins. J Recept Signal Tr R. 1995; 15:55–70.
62. Seifert R, Wenzel-Seifert K, Kobilka BK. GPCR-G alpha fusion proteins: molecular analysis of receptor-G-protein coupling. Trends Pharmacol Sci. 1999; 20:383–389. [PubMed: 10462762]

63. Trankle C, Weyand O, Schroter A, Mohr K. Using a radioalloster to test predictions of the cooperativity model for gallamine binding to the allosteric site of muscarinic acetylcholine M_2 receptors. Mol Pharmacol. 1999; 56:962–965. [PubMed: 10531401]
64. Lazareno S, Popham A, Birdsall NJM. Allosteric interactions of staurosporine and other indolocarbazoles with *N*-[methyl-^{3}H]scopolamine and acetylcholine at muscarinic receptor subtypes: Identification of a second allosteric site. Mol Pharmacol. 2000; 58:194–206. [PubMed: 10860942]
65. Trankle C, Mohr K. Divergent modes of action among cationic allosteric modulators of muscarinic M_2 receptors. Mol Pharmacol. 1997; 51:674–682. [PubMed: 9106634]
66. Potter LT, Ferrendelli CA, Hanchett HE, Hollifield MA, Lorenzi MV. Tetrahydroaminoacridine and other allosteric antagonists of hippocampal M_1 muscarine receptors. Mol Pharmacol. 1989; 35:652–660. [PubMed: 2725474]
67. Trankle C, Weyand O, Voigtländer U, Mynett A, Lazareno S, Birdsall NJM, Mohr K. Interactions of orthosteric and allosteric ligands with [^{3}H]dimethyl-W84 at the common allosteric site of muscarinic M_2 receptors. Mol Pharmacol. 2003; 64:180–190. [PubMed: 12815174]
68. Hoare SRJ, Strange PG. Regulation of D_2 dopamine receptors by amiloride and amiloride analogs. Mol Pharmacol. 1996; 50:1295–1308. [PubMed: 8913361]
69. Hoare SRJ, Coldwell MC, Armstrong D, Strange PG. Regulation of human D_1, D_2(long), D_2(short), D_3 and D_4 dopamine receptors by amiloride and amiloride analogues. Brit J Pharmacol. 2000; 130:1045–1059. [PubMed: 10882389]
70. Waelbroeck M. Identification of drugs competing with D-tubocurarine for an allostericsSite on cardiac muscarinic receptors. Mol Pharmacol. 1994; 46:685–692. [PubMed: 7969047]
71. Tucek S, Musilkova J, Nedoma J, Proska J, Shelkovnikov S, Vorlicek J. Positive cooperativity in the binding of alcuronium and *N*-methylscopolamine to muscarinic acetylcholine receptors. Mol Pharmacol. 1990; 38:674–680. [PubMed: 2233700]
72. Maass A, Mohr K. Opposite effects of alcuronium on agonist and on antagonist binding to muscarinic receptors. Eur J Pharmacol. 1996; 305:231–234. [PubMed: 8813558]
73. Kent RS, De LA, Lefkowitz RJ. A quantitative analysis of beta-adrenergic receptor interactions: Resolution of high and low affinity states of the receptor by computer modeling of ligand binding data. Mol Pharmacol. 1980; 17:14–23. [PubMed: 6104284]
74. Chidiac P, Wells JW. Effects of adenyl nucleotides and carbachol on cooperative interactions among G proteins. Biochemistry. 1992; 31:10908–10921. [PubMed: 1420202]
75. Lachance M, Ethier N, Wolbring G, Schnetkamp PP, Hebert TE. Stable association of G proteins with β_2AR is independent of the state of receptor activation. Cell Signal. 1999; 11:523–533. [PubMed: 10405763]
76. Ma AW, Pawagi AB, Wells JW. Heterooligomers of the muscarinic receptor and G proteins purified from porcine atria. Biochem Biophys Res Commun. 2008; 374:128–133. [PubMed: 18601900]

Abbreviations

CHL	cholesterol
DTT	dithiothreitol
GPCR	G protein-coupled receptor
HEPES	4-(2-hydroxyethyl)-1-piperazineethanesulfonic acid
PBS	phosphate-buffered saline
PMSF	phenylmethanesulfonyl fluoride
NMS	*N*-methylscopolamine
QNB	quinuclidinylbenzilate

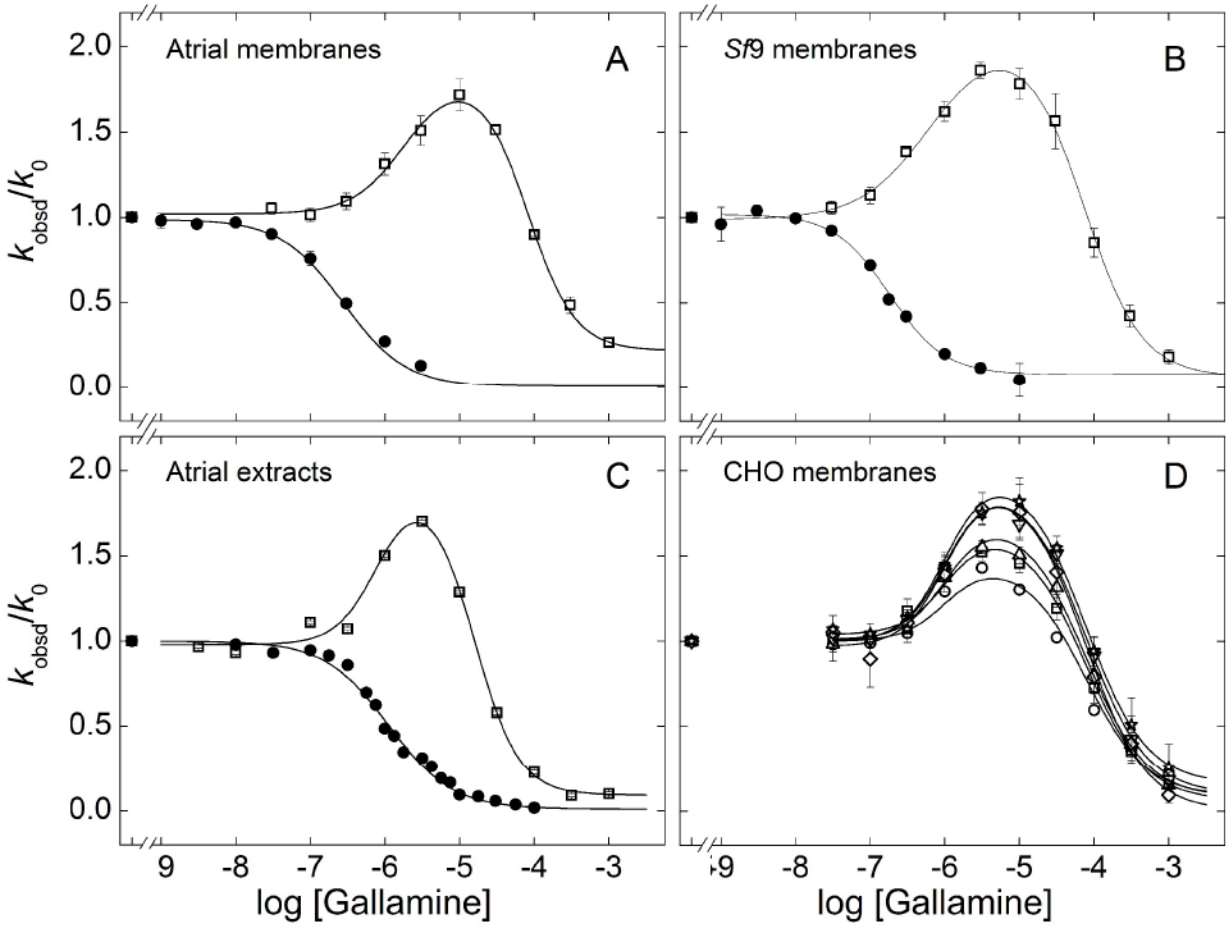

Figure 1.

Effect of gallamine on the rate of dissociation of *N*-[^{3}H]methylscopolamine and [^{3}H]quinuclidinylbenzilate. [^{3}H]QNB (open symbols) or [^{3}H]NMS (closed symbols) was incubated with M_2 receptor in sarcolemmal membranes from porcine atria (A), membranes from *Sf*9 cells (B), detergent-solubilized extracts from porcine sarcolemma (C), or membranes from CHO cells (D). The normalized rate of dissociation (k_{obsd}/k_0) was measured at graded concentrations of gallamine, and values at the same concentration were averaged to obtain the means (± S.E.M.) plotted on the *y*-axis. The lines depict the best fit of Equation 3 ($n = 1$, [^{3}H]NMS; $n = 2$, [^{3}H]QNB), and the parametric values are listed in Tables 1 (A–C) and 2 (D). The concentration of the radioligand in panels A–C was as follows: [^{3}H]NMS, 1.0 nM (A, B), 10 nM (C); [^{3}H]QNB, 0.20 nM (A, B), 1.0 nM (C). The concentration of [^{3}H]QNB (nM) in panel D was 0.02 (○), 0.04 (□), 0.20 (Δ), 1.0 (▽), 2.0 (◇), and 4.0 (☆).

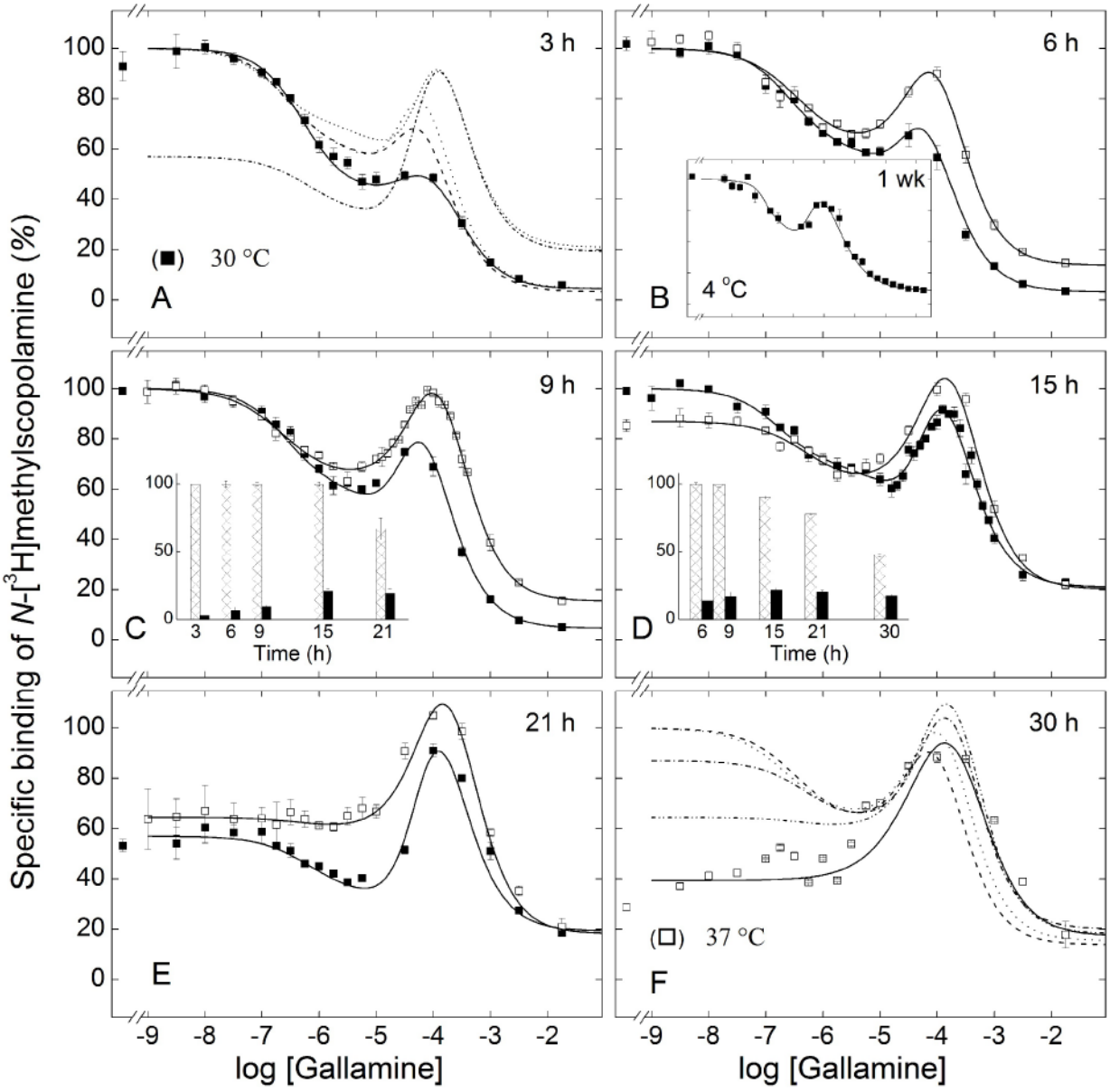

Figure 2.

Emergence of the effect of gallamine on the binding of *N*-[^{3}H]methylscopolamine to solubilized M_2 receptor from porcine atria. Gallamine and [^{3}H]NMS (10 nM) were mixed simultaneously with aliquots of the extract, and total binding was measured after incubation of the reaction mixture at either 30 °C (■) or 37 °C (□) for different times as follows: 3 h (A), 6 h (B), 9 h (C), 15 h (D), 21 h (E), and 30 h (F); total binding also was measured after incubation of the reaction mixture for 1 wk at 4 °C (B, inset). The solid lines depict the best fit of Equation 3 ($n = 3$) to all data acquired at the same temperature, and the parametric values are listed in Table 3. The fitted curves in panels B–E are reproduced as the broken lines in panels A (30 °C) and F (37 °C). The asymptotic values of Equation 3 at each time of incubation are compared in the insets to panels C (30 °C) and D (37 °C) ($Y_{[G]\rightarrow 0}$, hatched bars; $Y_{[G]\rightarrow\infty}$, solid bars). Details regarding the normalization of the data are described under 'Experimental Procedures.'

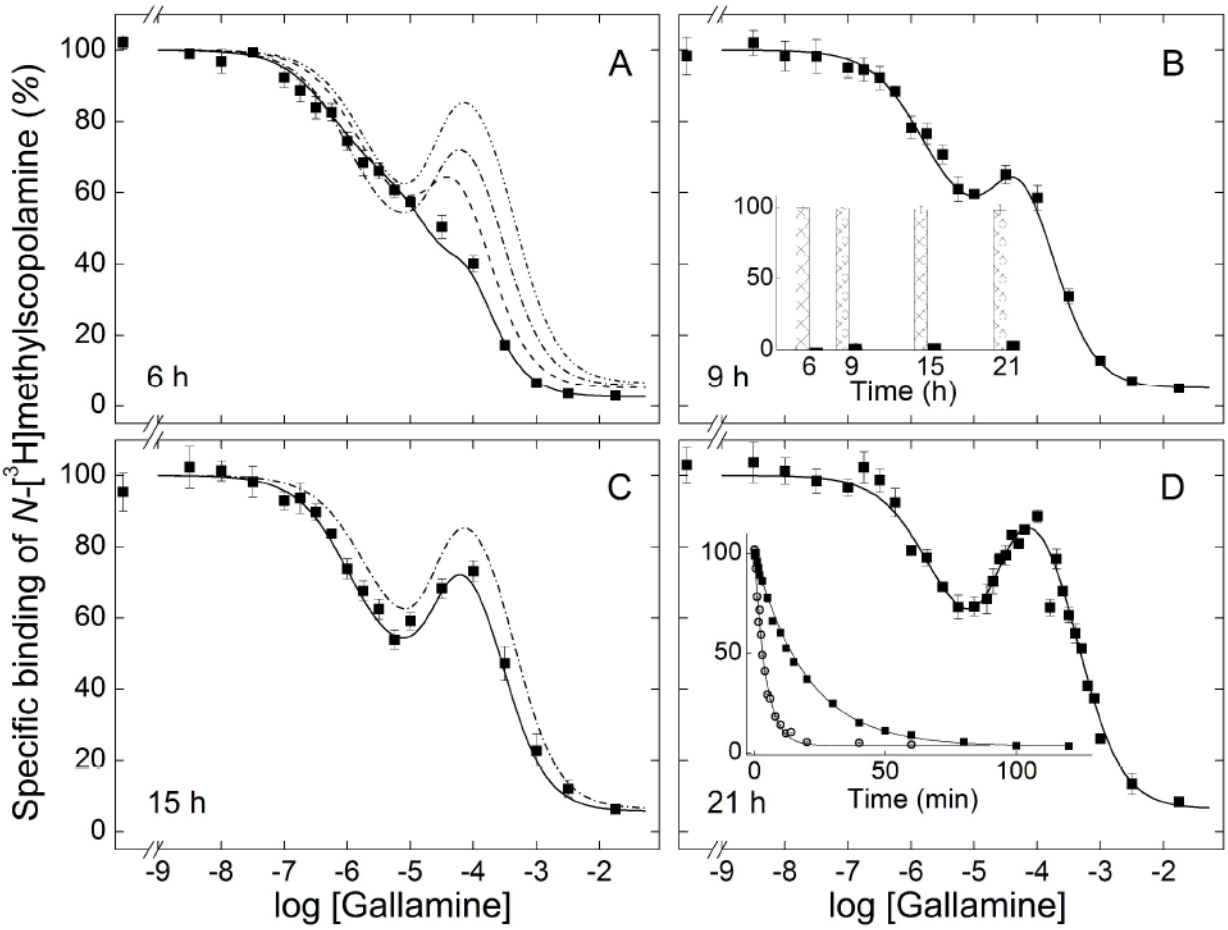

Figure 3.

Emergence of the effect of gallamine on the binding of *N*-[^{3}H]methylscopolamine to solubilized M_2 receptor from *Sf*9 cells. Gallamine and [^{3}H]NMS (10 nM) were mixed simultaneously with aliquots of the extract, and total binding was measured after incubation of the reaction mixture at 30 °C for 6 h (A), 9 h (B), 15 h (C), and 21 h (D). The solid lines depict the best fit of Equation 3 ($n = 3$) to the data represented in all panels taken together, and the parametric values are listed in Table 3. The fitted curves in panels B–D are reproduced as the broken lines in panel A; that from panel D is reproduced as the broken line in panel C. The asymptotic values of Equation 3 at each time of incubation are compared in the inset to panel B ($Y_{[G]\rightarrow 0}$, hatched bars; $Y_{[G]\rightarrow \infty}$, solid bars). The net dissociation of [^{3}H]NMS from receptor in extracts from *Sf*9 cells (■) and porcine atria (○) at 30 °C is shown in the inset to panel D. The lines represent the best fits of Equation 1, and the mean parametric values from all such experiments are as follows: *Sf*9 cells, $k = 0.053 \pm 0.002$ min $^{-1}$ ($N = 4$); porcine atria, $k = 0.17 \pm 0.01$ min $^{-1}$($N = 6$).

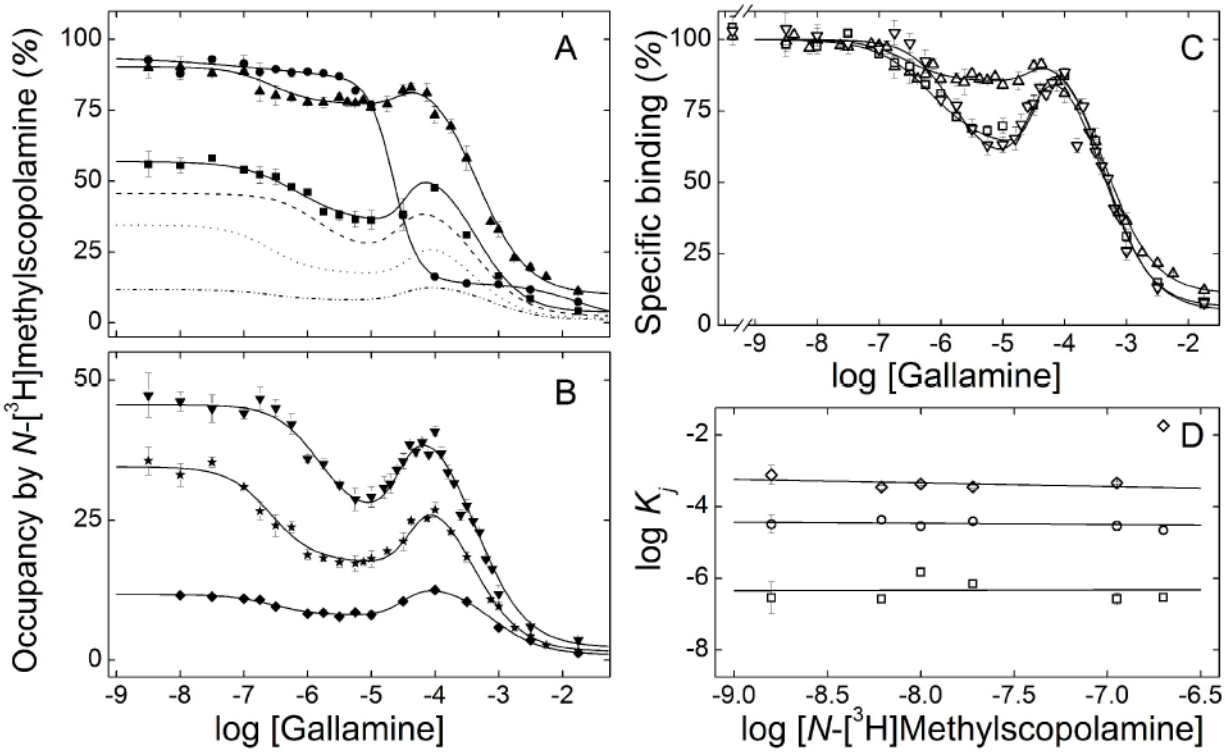

Figure 4.

Effect of the concentration of *N*-[^{3}H]methylscopolamine on the binding of gallamine to solubilized M_2 receptor from *Sf*9 cells. Gallamine and [^{3}H]NMS were mixed simultaneously with the solubilized extract, and total binding was measured after equilibration of the reaction mixture for 21 h at 30 °C. The concentrations of [^{3}H]NMS and the corresponding levels of occupancy in the absence of gallamine were as follows: (A) 200 nM and 94% (●), 112 nM and 90% (▲), 19.1 nM and 61% (■); (B) 10.1 nM and 46% (▼), 6.31 nM and 35% (★), 1.55 nM and 12% (◆). The solid lines depict the best fit of Equation 3 ($n = 3$) to all of the data represented in panels A and B taken together, and the parametric values are listed in Table 4. The fitted curves in panel B are reproduced as the broken lines in panel A. The data and fitted curves obtained at three concentrations of [^{3}H]NMS are reproduced in panel C [100 nM (Δ), 19.1 nM (○), 10 nM (▽)], normalized to the value of $Y_{[G]\rightarrow 0}$ taken as 100. The fitted values of log K_j obtained at each concentration of [^{3}H]NMS are shown in panel D (□, log K_1; ○, log K_2; ◇, log K_3). In each case, the slope of the line is indistinguishable from 0 ($P > 0.4$); the value of log K_3 at 200 nM [^{3}H]NMS was omitted from the calculation.

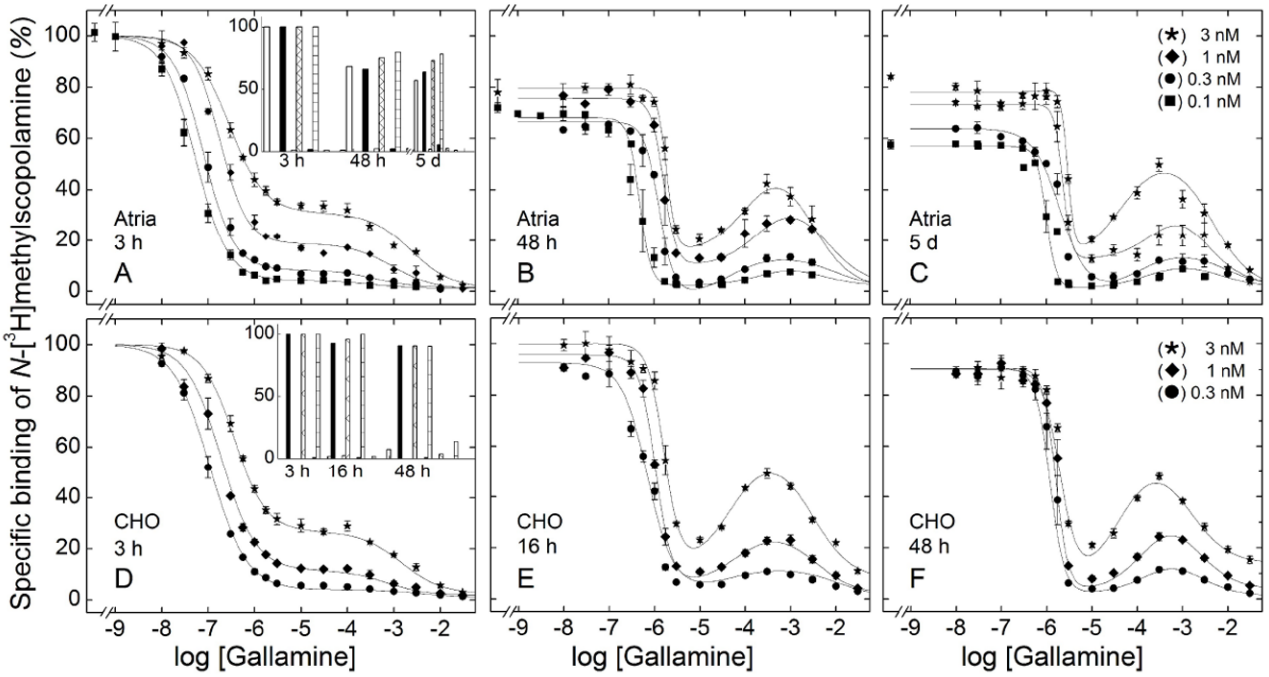

Figure 5.

Effect of the concentration of *N*-[^{3}H]methylscopolamine and the time of incubation on the binding of gallamine to M_2 receptor in mammalian membranes. Gallamine and [^{3}H]NMS were mixed simultaneously with membranes from porcine atria (A–C) or CHO cells (D–F), and total binding was measured after incubation of the reaction mixture at 24 °C for different times as follows: porcine atria, 3 h (A), 48 h (B), and 5 d (C); CHO cells, 3 h (D), 16 h (E), and 48 h (F). The concentrations of [^{3}H]NMS and the corresponding levels of occupancy in the absence of gallamine were as follows: 0.1 nM, 51.7% (●); 0.3 nM, 76.4% (■); 1 nM, 91.5% (◆); 3 nM, 97% (★). The lines represent the best fits of Equation 3 (n = 2 or 3) to the data, and the parametric values are listed in Table S7. The asymptotic values of Equation 3 at each time of incubation are compared in the insets to panels A (atrial membranes) and D (CHO membranes) ($Y_{[G]\rightarrow 0}$, longer bars; $Y_{[G]\rightarrow \infty}$, shorter bars). The concentration of [^{3}H]NMS was as follows, from left to right: open bars, 0.1 nM; solid bars, 0.3 nM; hatched bars, 1 nM, and checkered bars, 3 nM.

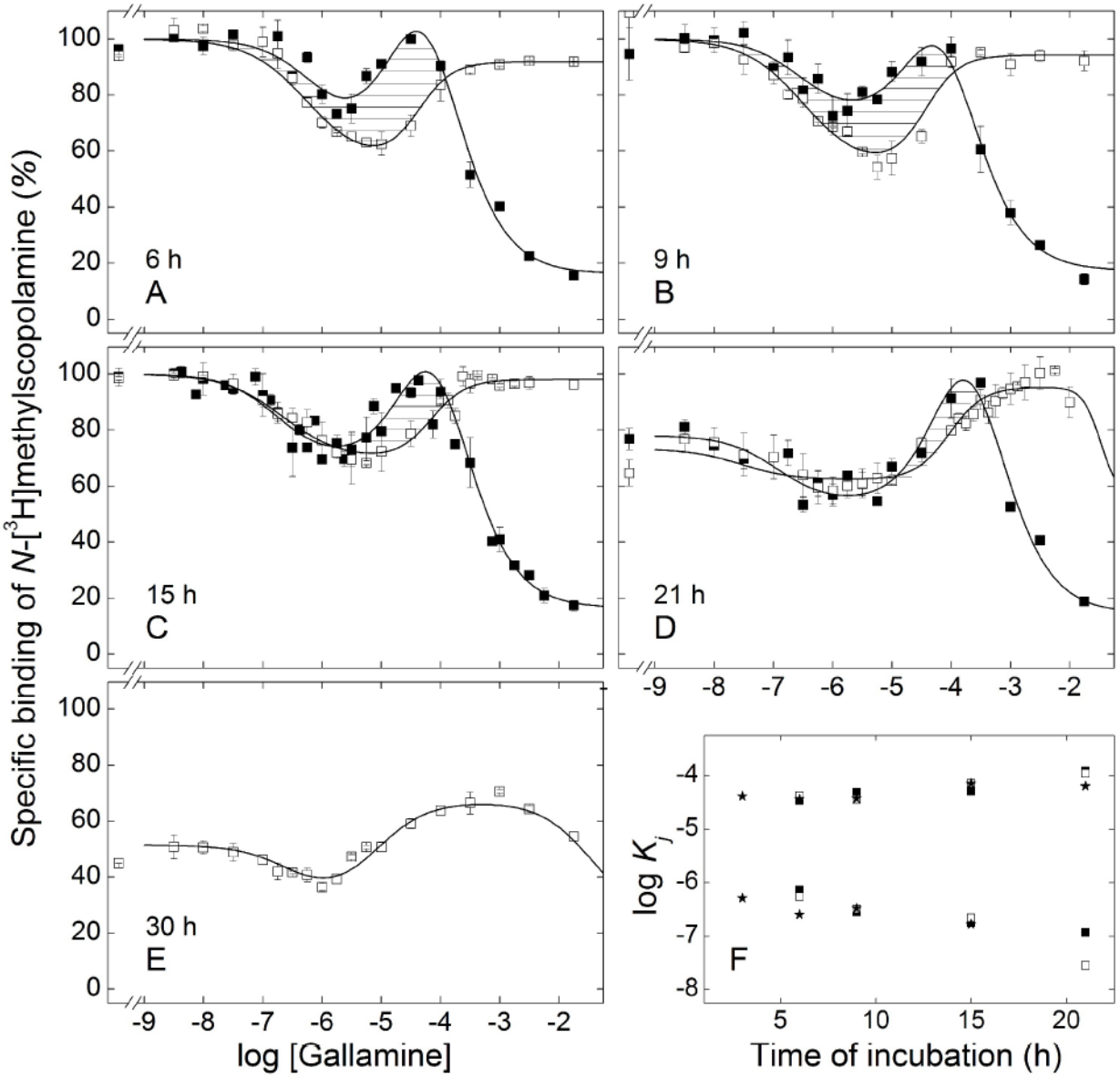

Figure 6.

Effect of the order of mixing on the equilibration of gallamine and *N*-[^{3}H]methylscopolamine with solubilized M_2 receptor from porcine atria. Aliquots of the extract were premixed with [^{3}H]NMS at a concentration of 10 nM (□) or with gallamine at the concentrations shown on the abscissa (■), and the mixture was incubated for 2 h at 30 °C. The second ligand then was added, and total binding was measured after further incubation at 30 °C for different times as follows: 6 h (A), 9 h (B), 15 h (C), 21 h (D), and 30 h (E). The lines depict the best fit of Equation 3 (n = 2 or 3) to the data represented in panels A–D taken together or to the data represented in Panel E, and the parametric values are listed in Table 5. Details regarding the normalization of the data are described under 'Experimental Procedures.' The estimates of log K_j obtained for different orders of mixing are compared in panel F (★, simultaneous addition of gallamine and [^{3}H]NMS; ■, prior addition of gallamine; □ prior addition of [^{3}H]NMS). Values shown for the simultaneous

addition of gallamine and [^{3}H]NMS are from Table 3; those for sequential addition are from Table 5.

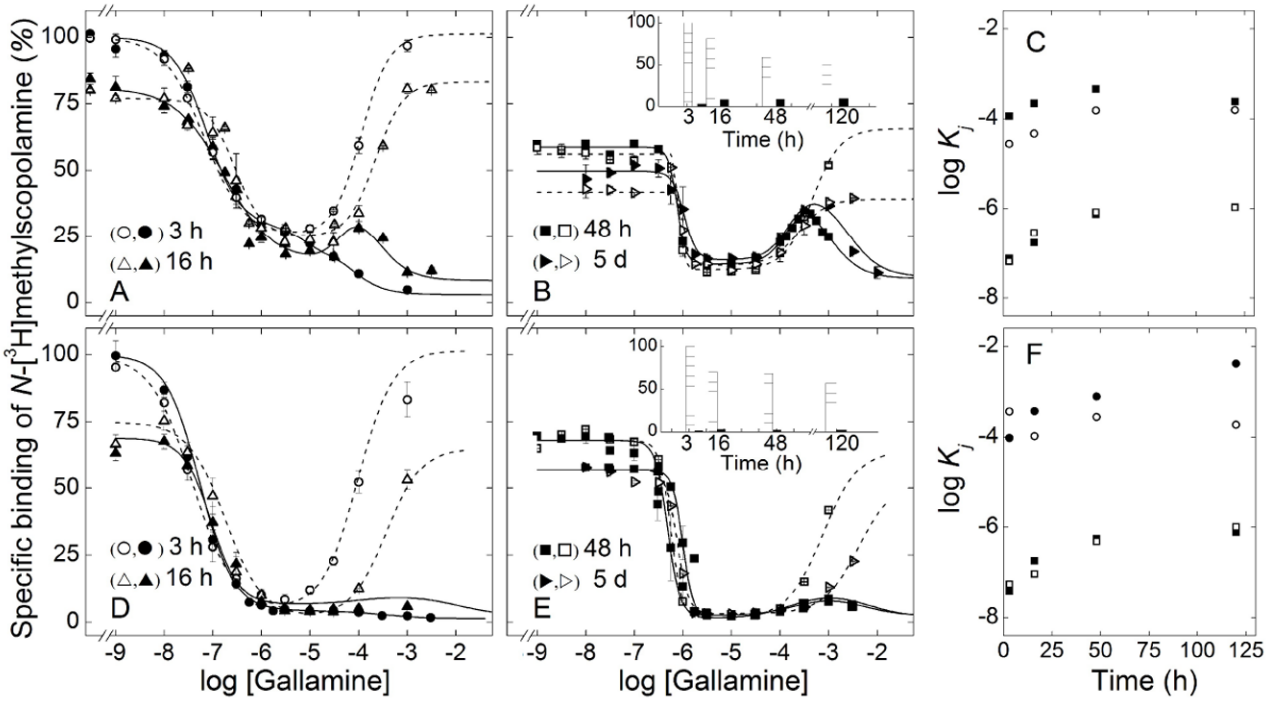

Figure 7.

Effect of the order of mixing on the equilibration of gallamine and *N*-[^{3}H]methylscopolamine with M_2 receptor in membranes from porcine atria and *Sf*9 cells. Membranes from *Sf*9 cells (A, B) or porcine atria (D, E) were mixed simultaneously with gallamine and [^{3}H]NMS (0.3 nM) (closed symbols) or first with [^{3}H]NMS (0.3 nM) and then with gallamine after incubation of the initial mixture for 30 min at 24 °C (open symbols). Total binding was measured after further incubation at 24 °C for different times as follows: 3 h○,(●) and 16 h (Δ,▲) (A, D), 48 h (□,■) and 5 d (▷,▶) (B, E). The lines depict the best fit of Equation 3 (n = 2 or 3) to data obtained after simultaneous mixing (solid lines) or after premixing with [^{3}H]NMS (broken lines), and the parametric values are listed in Table S10. The asymptotic values of Equation 3 for each time of incubation after simultaneous mixing with are compared in the insets to panels B (Sf9 cells) and E (atria) ($Y_{[G]\rightarrow 0}$, hatched bars; $Y_{[G]\rightarrow \infty}$, solid bars). The fitted values of log K_j from Table S10 are shown in panels C (*Sf*9 cells) and F (atria) for log K_1 (□,■) and log K_2 (○,●) after simultaneous mixing (■,●) and premixing with [^{3}H]NMS (□,○).

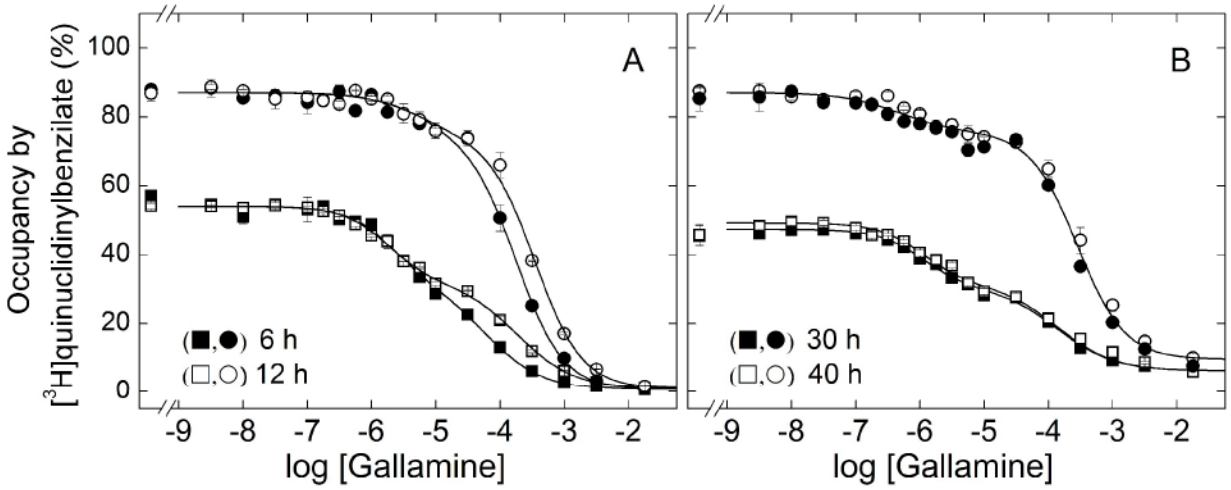

Figure 8.

Effect of the concentration of [^{3}H]quinuclidinylbenzilate and the time of incubation on the binding of gallamine to solubilized M_2 receptor from *Sf*9 cells. Gallamine and [^{3}H]QNB were added simultaneously to aliquots of the solubilized extract, and total binding was measured after incubation of the reaction mixture at 30 °C for different times as follows: 6 h (■, ●) and 12 h (□,○) (A), 30 h (■, ●) and 40 h (□,○) (B). The concentrations of [^{3}H]QNB and the corresponding levels of occupancy were as follows: 3.9 nM, 54% (■,□); 22 nM, 87 % (●,○). The lines represent the best fit of Equation 3 (n = 2) to the pooled data at each level of occupancy, and the parametric values are listed in Table 6.

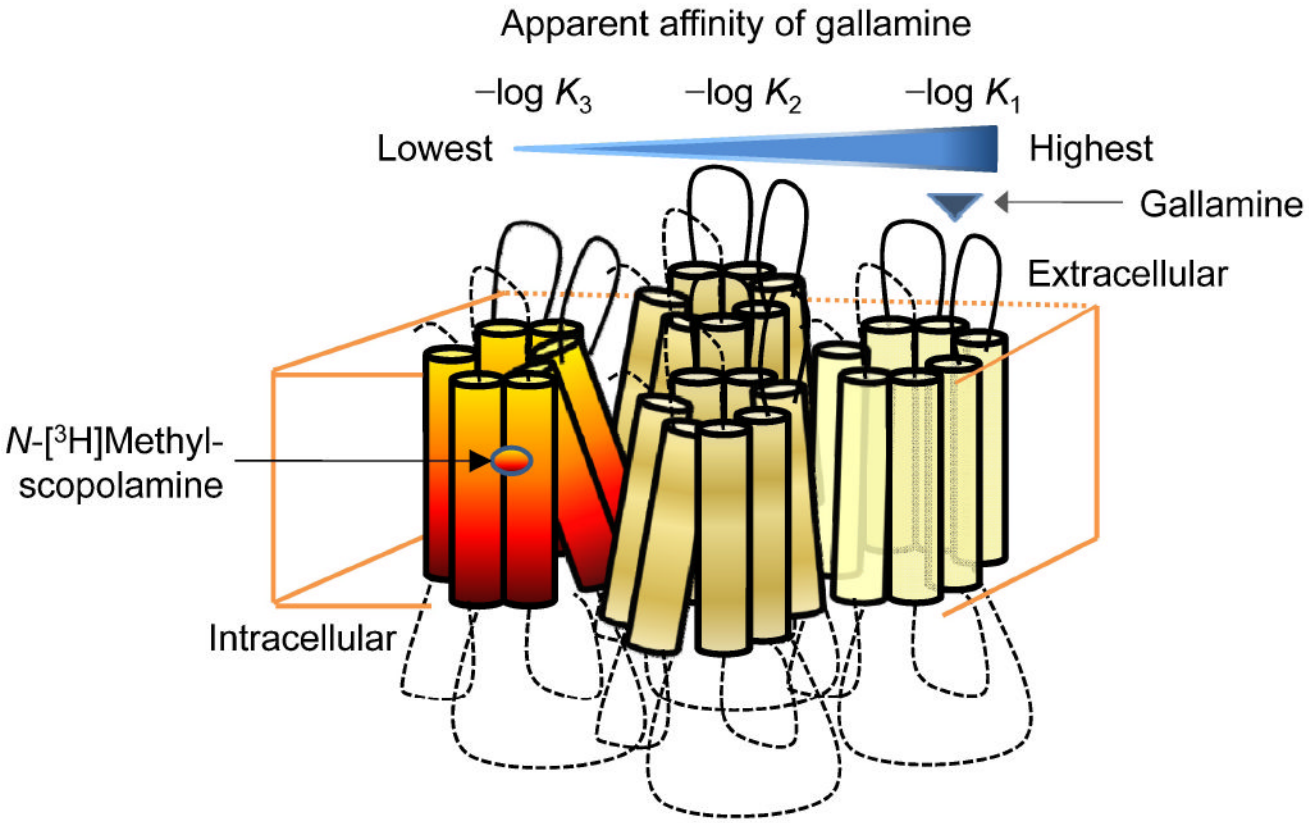

Figure 9.

Heterogeneity induced by *N*-[^{3}H]methylscopolamine among the allosteric sites of an oligomer. Binding of [^{3}H]NMS to a tetramer configured as a square or a rhombus gives rise to a conformational asymmetry characterized by three classes of protomer: those occupied by [^{3}H]NMS (red–yellow), those adjacent to protomers occupied by [^{3}H]NMS (yellow), and those diagonally opposite protomers occupied by [^{3}H]NMS (light yellow). Gallamine binds with highest apparent affinity to the allosteric site of an otherwise vacant protomer that is most distant from a single protomer occupied by [^{3}H]NMS (*i.e.*, log K_1). It binds with lowest apparent affinity to the allosteric site of a protomer in which the local orthosteric site is occupied by [^{3}H]NMS (*i.e.*, log K_3).

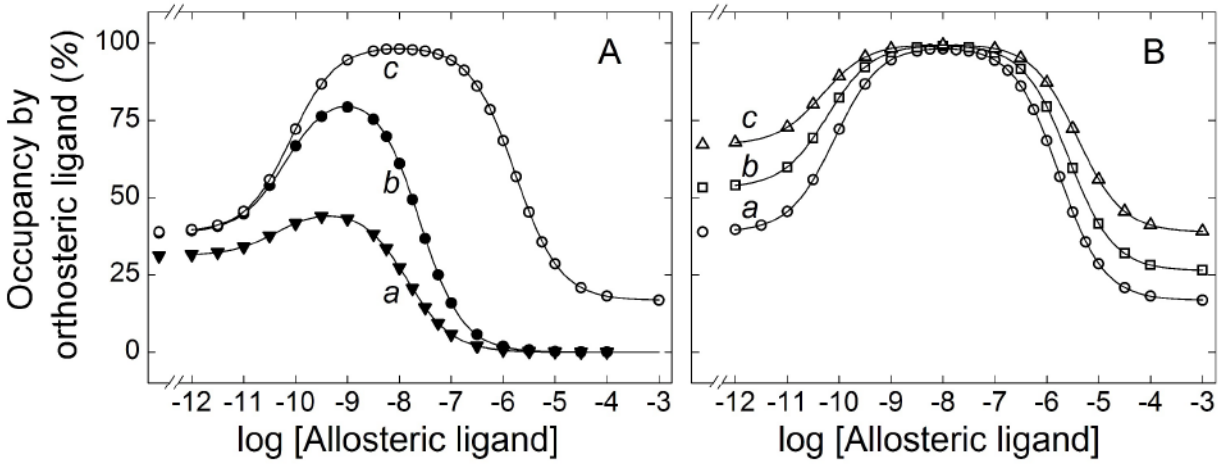

Figure 10.

Effect of time and the concentration of an orthosteric probe on allosteric interactions within a dimeric receptor. The points were simulated according to Scheme 3 and depict total specific binding of an orthosteric ligand in the presence of an allosteric ligand at graded concentrations of the latter. There is no binding at t = 0 (*i.e.*, R_{OO}^{OO}=100% of the receptor in Scheme 3), and the simulations therefore depict an arrangement in which the two ligands are mixed simultaneously with the receptor. The amount of each species of receptor was computed with the parametric values listed in Table S14 to obtain the value of total bound L plotted on the ordinate (*i.e.*, $R_{OL}^{OO}+R_{LO}^{OO}+2R_{LL}^{OO}+R_{OL}^{AO}+\cdots+2R_{LL}^{AA}$). Further details are described in the supporting information. (A) Total binding 5 min after mixing (▼), 15 min after mixing (●), and at equilibrium (○). The apparent level of occupancy by L in the absence of A at equilibrium is 38.7% ([L] = 316 nM). (B) Total binding at equilibrium for different levels of occupancy by L in the absence of A: 38.7%, [L] = 316 nM (○); 52.9%, [L] = 562 nM (□), and 66.7%, [L] = 1,000 nM (Δ). The lines in each panel depict the best fits of Equation 3 (n = 2) to the simulated data, and the parametric values are listed in Table S15.

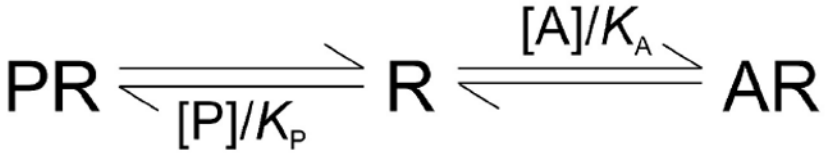

Scheme 1.

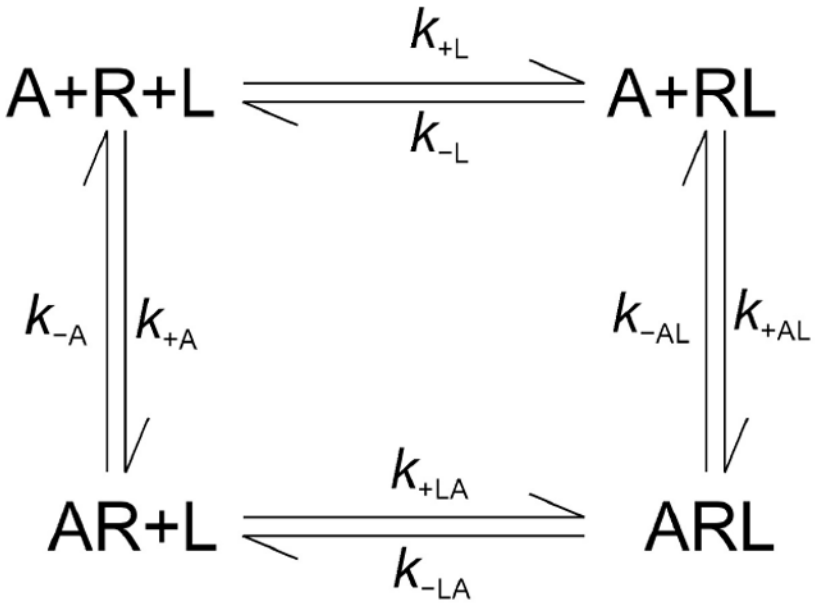

Scheme 2.

Heterotropic cooperativity within a monomeric receptor. A receptor (R) binds an allosteric ligand (A) and an orthosteric ligand (L) at topographically distinct sites to form a binary complex with either ligand (AR and RL) or a ternary complex with both (ARL). The first- and second order rate constants for binding to the vacant receptor are $k_{\pm A}$ and $k_{\pm L}$; those for binding to a ligand-occupied receptor are $k_{\pm AL}$ and $k_{\pm LA}$. Details regarding the simulations in terms of Scheme 2 are described in the supporting information (pp. S-2–S-4).

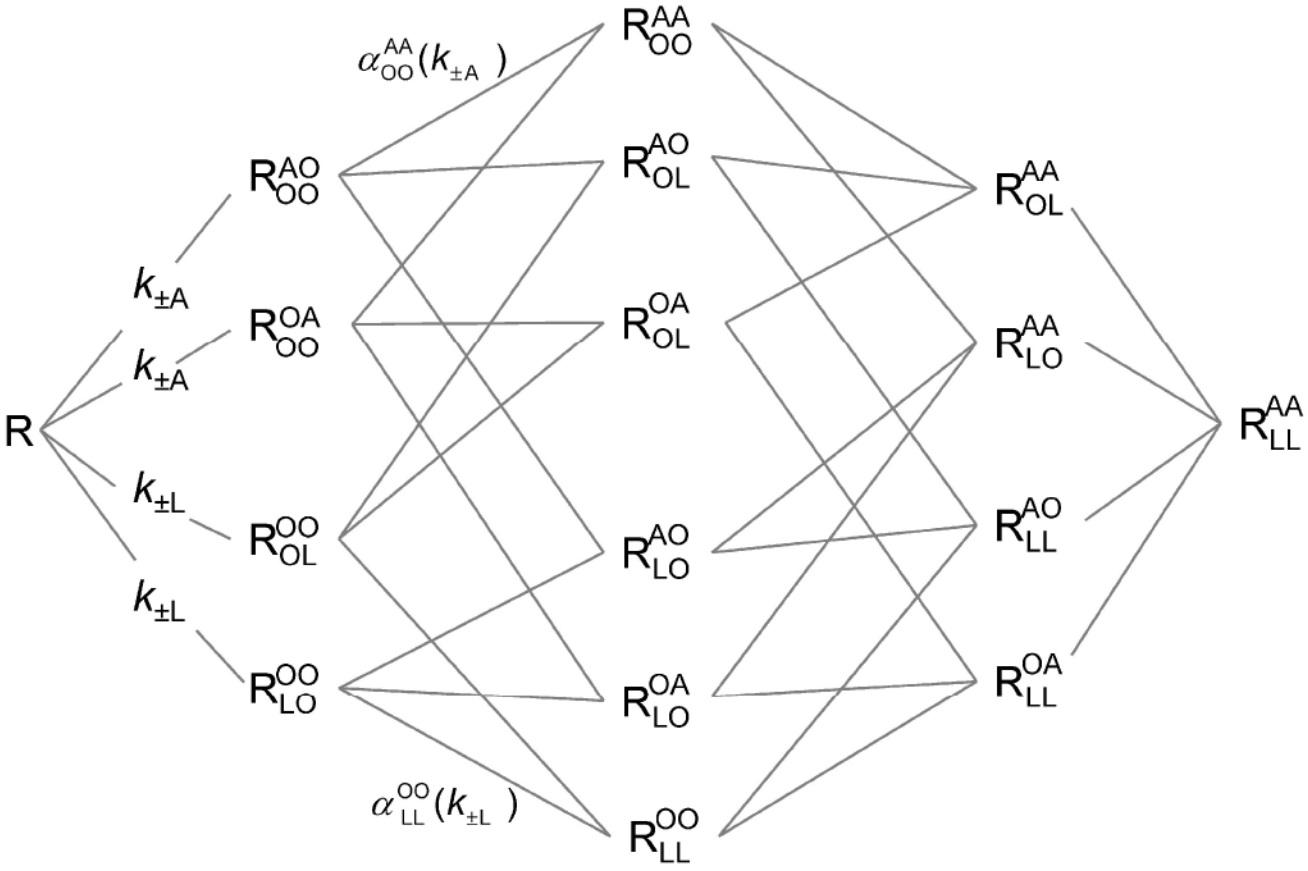

Scheme 3.

Homo- and heterotropic cooperativity within a dimeric receptor. Each protomer of a dimeric receptor (R) contains one allosteric site and one orthosteric site, each of which may be vacant (O) or occupied by the relevant ligand (A or L). The state of occupancy is indicated by a superscript (allosteric site) and a subscript (orthosteric site) in which the first and second positions denote protomers 1 and 2, respectively. The first- and second order rate constants for binding to the vacant receptor are $k_{\pm A}$ and $k_{\pm L}$. Rate constants for the binding of additional ligands are determined by the values of $k_{\pm A}$, $k_{\pm L}$, and the relevant cooperativity factors (α). The cooperativity factor associated with each species of receptor is identified by a superscript and a subscript that denotes the state of occupancy as described above. Two such factors are illustrated in the Scheme (*i.e.*, α^{AA}_{OO} and α^{OO}_{LL}). Further details are described in the supporting information (pp. S-4–S-8).

Table 1

Parametric Values for the Effect of Gallamine on the Rate of Dissociation of *N*-[^{3}H]Methylscopolamine and [^{3}H]Quinuclidinylbenzilate[a]

radioligand, preparation	[P][e] (nM)	log K_1	log K_2	$n_{H(1)}$	$n_{H(2)}$	F_1	F_2	k_{obsd}/k_0 [G] = 0	k_{obsd}/k_0 [G]→∞
[^{3}H]NMS									
Atria, M (3)[b]	1.0	−6.56 ± 0.07		1.04 ± 0.13		1.00	*f*	0.99 ± 0.01	0.07 ± 0.05
*Sf*9, M (4)[c]	1.0	−6.74 ± 0.03		1.18 ± 0.11		1.00	*f*	1.01 ± 0.01	0.08 ± 0.02
Atria, S (6)[d]	10	−5.95 ± 0.04		1.02 ± 0.08		1.00	*f*	1.00 ± 0.02	0.01 ± 0.01
[^{3}H]QNB									
Atria, M (2)	0.02	−5.94 ± 0.19	−4.10 ± 0.09	1.27 ± 0.37[g]	1.35 ± 0.25[g]	−0.99	1.99 ± 0.23	0.95 ± 0.04	0.15 ± 0.08
Atria, M (5)[b]	0.20	−5.82 ± 0.16	−4.07 ± 0.07			−0.98	1.98 ± 0.20	1.00 ± 0.03	0.23 ± 0.06
*Sf*9, M (4)[c]	0.20	−5.99 ± 0.31	−4.35 ± 0.30	0.97 ± 0.30	0.80 ± 0.14	−1.51	2.51 ± 0.82	1.02 ± 0.04	0.00 ± 0.00
Atria, S (3)[d]	1.0	−6.04 ± 0.15	−4.83 ± 0.13	1.85[h] ± 0.15	1.36 ± 0.28	−1.12	2.12 ± 0.39	0.99 ± 0.03	0.08 ± 0.04

[a] Estimates of k_{obsd}/k_0 at graded concentrations of gallamine were obtained for receptor in membranes (M) and solubilized extracts (S) from porcine atria and *Sf*9 cells. The data were analyzed in terms of Equation 3 (n = 1 or 2) to obtain the parametric values listed in the table and the fitted curves shown in Figure 1. Values in parentheses indicate the total number of experiments, where each experiment included measurements at four or more concentrations of gallamine and a control in the absence of gallamine.

[b] Figure 1A.

[c] Figure 1B.

[d] Figure 1C.

[e] The concentration of the radioligand (P ≡ [^{3}H]NMS or [^{3}H]QNB).

[f] A single class of sites is sufficient to describe the data (*i.e.*, n = 1).

[g] There is no significant difference in the sum of squares with single rather than separate values of $n_{H(j)}$ for data acquired at the two different concentrations of [^{3}H]QNB (P = 0.55).

[h] The value significantly exceeds 1 (P = 0.04).

Table 2

Parametric Values for the Effect of Gallamine on the Rate of Dissociation of [^{3}H]Quinuclidinylbenzilate from Receptor in CHO Membranes at Different Concentrations of the Radioligand[a]

[^{3}H]QNB [b]								k_{obsd}/k_0	
(nM)	(%)	log K_1	log K_2	$n_{H(1)}$	$n_{H(2)}$	F_1	F_2	[G] = 0	[G]→∞
0.02	48 (8)	−5.99 ± 0.07	−4.11 ± 0.05	1.54 ± 0.31	1.07 ± 0.11	−0.52	1.52 ± 0.10	1.00 ± 0.03	0.09 ± 0.06
0.04	65 (4)					−0.64	1.64 ± 0.13	1.04 ± 0.04	0.06 ± 0.07
0.2	90 (9)					−0.78	1.78 ± 0.12	1.01 ± 0.03	0.08 ± 0.06
1.0	98 (9)					−1.06	2.06 ± 0.14	1.00 ± 0.03	0.10 ± 0.06
2.0	99 (4)					−1.02	2.02 ± 0.16	0.97 ± 0.05	0[c]
4.0	99 (3)					−1.21	2.21 ± 0.21	1.00 ± 0.05	0.16 ± 0.09

[a] The data represented in Figure 1D were pooled and analyzed in terms of Equation 3 (n = 2) to obtain the fitted parametric values listed in the table and the fitted curves shown in the figure. Single values of log K_1, log K_2, $n_{H(1)}$, and $n_{H(2)}$ were common to all of the data. There was no significant difference in the sum of squares over that obtained with separate values of each parameter for the data at each concentration of [^{3}H]QNB (P = 0.8). The number of independent experiments is shown in parentheses.

[b] The level of occupancy was calculated as [P]/([P] + K), where [P] is the concentration of [3H]QNB. The value of K was taken as 0.022 nM (Table S1).

[c] The asymptotic value of k_{obsd}/k_0 as [G]→∞ is indistinguishable from zero and was fixed accordingly.

Table 3

Parametric Values for the Effect of Temperature and Time of Incubation on the Binding of *N*-[^{3}H]Methylscopolamine and Gallamine to Solubilized M_2 Receptor from Porcine Atria and *Sf*9 Cells[a]

time	log K_1	log K_2	log K_3	$n_{H(1)}$	$n_{H(2)}$	$n_{H(3)}$	F_1	F_2	F_3
extract from porcine atria at 4 °C (Figure 2B, inset)									
7 d (2)	−6.94 ± 0.14	−5.44 ± 0.07	−5.12 ± 0.12	2.75[b] ± 2.49	1.59[a] ± 0.19	0.75 ± 0.07	0.22	−1.52 ± 0.12	2.30[c]
extract from porcine atria at 30 °C (Figure2A–F)									
3 h (5)	−6.29 ± 0.08	−4.39 ± 0.28	−3.67 ± 0.27	1.11 ± 0.17	1.49[b] ± 0.07	1.10 ± 0.06	0.60	−0.33 ± 0.33	0.73 ± 0.33
6 h (5)	−6.60 ± 0.17	−4.44 ± 0.08	−4.18 ± 0.19				0.40	−1.66 ± 0.97	2.26 ± 1.03
9 h (6)	−6.48 ± 0.17	−4.43 ± 0.07	−4.18 ± 0.17				0.41	−2.32 ± 1.10	2.92 ± 1.16
15 h (8)	−6.78 ± 0.24	−4.15 ± 0.05	−3.94 ± 0.05				0.39	−3.38 ± 0.04	4[d]
21 h (2)	−6.21 ± 0.24	−4.21 ± 0.05	−3.87 ± 0.06	1.00[c]			0.57	−6.52 ± 0.11	6.95[e]
extract from porcine atria at 37 °C (Figures 2A–F)									
6 h (4)	−6.45 ± 0.18	−4.17 ± 0.11	−3.93 ± 0.50	0.95 ± 0.17	1.22 ± 0.08	1.16 ± 0.05	0.46	−3.25 ± 8.54	3.79 ± 8.59
9 h (6)	−6.66 ± 0.15	−4.06 ± 0.10	−3.79 ± 0.10				0.42	−3.42 ± 0.05	4[d]
15 h (6)	−6.29 ± 0.17	−3.96 ± 0.08	−3.62 ± 0.08	1.00[c]			0.38	−3.77 ± 0.06	4.39[e]
21 h (2)	−4.25 ± 0.17	−3.97 ± 0.14	−3.48 ± 0.45	1.00[c]			0.31	−3.79 ± 21.3	5.10[e]
extract from *Sf*9 cells at 30 °C (Figures 3A–D)									
6 h (3)	−6.26 ± 0.22	−4.26 ± 0.16	−4.19 ± 0.18	1.06 ± 0.21	1.82[b] ± 0.49	1.25 ± 0.09	0.36	−0.98 ± 0.97	1.62 ± 1.02
9 h (5)	−5.81 ± 0.20	−4.60 ± 0.21	−3.81 ± 0.15				0.53	−0.39 ± 0.20	0.86 ± 0.20
15 h (5)	−5.98 ± 0.17	−4.56 ± 0.14	−3.56 ± 0.09				0.58	−0.49 ± 0.15	0.91 ± 0.13
21 h (4)	−5.69 ± 0.26	−4.59 ± 0.11	−3.36 ± 0.21				0.56	−0.56 ± 0.18	1[d]

[a] The data represented in Figures 2 and 3 were analyzed in terms of Equation 3 (n = 3) to obtain the parametric values listed in the table. Data from the same preparation at the same temperature were analyzed in concert. Single values of $n_{H(2)}$ and $n_{H(3)}$ were shared by all of the data irrespective of the time of incubation, as indicated by the brackets. A single value of $n_{H(1)}$ was shared by all data obtained while the receptor remained stable; when there was a time-dependent loss of binding, the value was fixed at 1. The constraints on $n_{H(j)}$ were without significant effect on the sum of squares ($P > 0.9$). Single values of log K_j were common to data acquired after the same period of incubation. The number of independent experiments is shown in parentheses.

[b] The value significantly exceeds 1 ($P < 0.01$)

[c] The value is indistinguishable from 1 ($P = 0.90$) and was fixed accordingly during successive iterations of the fitting procedure.

[d] The value is defined by a shallow minimum in the sum of squares, as determined by mapping, and was fixed accordingly.

[e] The value was fixed to compensate for the time-dependent decrease in $Y_{[G]=0} - Y_{[G]\to\infty}$ at low concentrations of gallamine, based on the assumption that the intrinsic maximum was the same as that after the attainment of equilibrium but before the onset of instability (*i.e.*, after 15 h at 30 °C, after 9 h at 37 °C).

Table 4

Parametric Values for the Effect of *N*-[^{3}H]Methylscopolamine on the Binding of Gallamine to Solubilized M_2 Receptor from *Sf*9 Cells[a]

[^{3}H]NMS[b]										
(nM)	(%)	log K_1	log K_2	log K_3	$n_{H(1)}$	$n_{H(2)}$	$n_{H(3)}$	F_1	F_2	F_3
1.55	11.7 (2)	−6.54 ± 0.44	−4.49 ± 0.25	−3.12 ± 0.27				0.56	−0.56 ± 0.25	1.22 ± 0.25
6.31	34.5 (4)	−6.58 ± 0.09	−4.37 ± 0.06	−3.46 ± 0.04				0.51	−0.51 ± 0.03	1[e]
10.1	45.5 (6)	−5.83 ± 0.12	−4.55 ± 0.06	−3.37 ± 0.03	1.29 ± 0.20	2.31 ± 0.44[b]	1.10 ± 0.05	0.46	−0.46 ± 0.06	1[e]
19.1	61.4 (2)	−6.15 ± 0.11	−4.41 ± 0.08	−3.45 ± 0.04				0.40	−0.40 ± 0.04	1[e]
112	90.3 (4)	−6.57 ± 0.16	−4.54 ± 0.13	−3.34 ± 0.03				0.16	−0.16 ± 0.02	1[e]
200	94.3 (2)	−6.53 ± 2.65	−4.65 ± 0.02	−1.75 ± 1.03	0.40 ± 0.40	2.28 ± 0.34[c]	1[d]	0.10	0.76 ± 0.17	0.14 ± 0.10

[a] The data represented in Figure 4 were analyzed in terms of Equation 3 (n = 3) to obtain the parametric values listed in the table. All of the data acquired at and below 100 nM [^{3}H]NMS were analyzed in concert, with single values of $n_{H(j)}$ as indicated by the brackets. Single values of log K_j were common to data acquired at the same concentration of [^{3}H]NMS. The constraints on $n_{H(j)}$ were without significant effect on the sum of squares ($P > 0.42$). The number of independent experiments is shown in parentheses.

[b] The concentration of [^{3}H]NMS is the mean from all experiments represented in the analysis (S.E.M./μ < 0.47). The corresponding level of occupancy was calculated as [P]/([P] + K), with the value of K taken as 10 nM (Table S1).

[c] The value significantly exceeds 1 ($P < 0.00001$).

[d] The value is indistinguishable from 1 ($P = 0.61$) and was fixed accordingly.

[e] The value was mapped to reveal a shallow minimum near 1 in the sum of squares and was fixed accordingly.

Table 5

Parametric Values for the Effect of the Order of Mixing on the Equilibration of Gallamine and *N*-[^{3}H]Methylscopolamine with Solubilized M_2 Receeptor from Porcine Atria[a]

time[b]	log K_1	log K_2	log K_3	$n_{H(1)}$	$n_{H(2)}$	$n_{H(3)}$	F_1	F_2	F_3
after premixing the receptor and gallamine									
6 h (2)	−6.13 ± 0.63	−4.47 ± 0.27	−4.12 ± 0.24	1[c]			0.42	−3.42 ± 0.31	4[e]
9 h (2)	−6.55 ± 0.36	−4.32 ± 0.25	−4.02 ± 0.24	1[c]			0.33	−3.33 ± 0.11	4[e]
15 h (3)	−6.75 ± 0.28	−4.29 ± 0.24	−3.96 ± 0.22	1[c]	1.02 ± 0.14	0.95 ± 0.09	0.37	−3.37 ± 0.09	4[e]
21 h (2)	−6.93 ± 0.84	−3.92 ± 0.25	−3.53 ± 0.22	1[c]			0.38	−4.27 ± 0.11	4.89[f]
after premixing the receptor and [^{3}H]NMS									
6 h (2)	−6.26 ± 0.20	−4.38 ± 0.17	—	0.88 ± 0.17	1.50[f] ± 0.16	—	—	*h*	*i*
9 h (2)	−6.49 ± 0.21	−4.44 ± 0.18	—			—	—	*h*	*i*
15 h (3)	−6.66 ± 0.10	−4.16 ± 0.09	—			—	—	*h*	*i*
21 h (3)	−7.55 ± 0.15	−4.03 ± 0.03	−1.48 ± 15.9	1[d]		2.86 ± 0.20	—	—	—
30 h (3)	−6.22 ± 0.43	−4.67 ± 0.32	−1.47 ± 1.52	1[d]	1[d]	1[d]	—	—	—

[a] The data represented in Figure 6 were analyzed in terms of Equation 3 (n = 2 or 3) to obtain the parametric values listed in the table. Data obtained following the same order of mixing were analyzed in concert; those obtained after different periods of incubation shared single values of $n_{H(j)}$ where indicated by the brackets. The number of independent experiments is shown in parentheses.

[b] Time of incubation after addition of the second ligand.

[c] The value is not well defined and was fixed at 1; there is no appreciable effect on the sum of squares ($P > 0.9$).

[d] The value is indistinguishable from 1 ($P = 0.51$) and was fixed accordingly owing to the time-dependent decrease in binding at low concentrations of gallamine.

[e] The value is defined by a shallow minimum in the sum of squares, as defined by mapping, and was fixed accordingly.

[f] The value was adjusted to compensate for the time-dependent decrease in binding at low concentrations of gallamine.

[g] The value significantly exceeds 1 ($P = 0.0009$).

[h] Owing to the small difference in value between $Y_{[G]\to 0}$ and $Y_{[G]\to\infty}$, the value of F_2 is comparatively large.

[i] Two classes of sites (n = 2).

Table 6

Parametric Values for the Effect of [^{3}H]Quinuclidinylbenzilate and the Time of Incubation of the Binding of Gallamine to Solubilized M_2 Receptor from *Sf*9 Cells[a]

[^{3}H]QNB[b]									
(nM)	(%)	time	log K_1	log K_2	Δ(log K)[c]	$n_{H(2)}$	$n_{H(2)}$	F_1	F_2
3.89	54	6 h (2)	−5.68 ± 0.05	−4.20 ± 0.05	1.48				
3.89	54	12 h (2)	−5.74 ± 0.07	−3.72 ± 0.06	2.02				
3.89	54	30 h (4)	−5.95 ± 0.06	−3.85 ± 0.05	2.10	1.23 ± 0.02	0.99 ± 0.05	0.41	0.59 ± 0.02
3.89	54	40 h (4)							
22.4	87	6 h (2)	−5.18 ± 0.25	−3.74 ± 0.02	1.44				
22.4	87	12 h (2)	−5.24 ± 0.26	−3.45 ± 0.05	1.79				
22.4	87	30 h (4)	−6.34 ± 0.17	−3.55 ± 0.05	2.79	1.00[d]	1.19 ± 0.01	0.15	0.85 ± 0.01
22.4	87	40 h (4)							

[a] The data represented in Figure 8 were analyzed in terms of Equation 3 (n = 2) to obtain the parametric values listed in the table. Data obtained at the same concentration of [^{3}H]QNB were analyzed in concert. Within each analysis, data obtained after all periods of incubation shared single values of $n_{H(j)}$; data obtained after incubation for 30 h and 40 h also shared single values of log K_j. The constraints on $n_{H(j)}$ and log K_j were without appreciable effect on the sum of squares ($P > 0.05$). The number of independent experiments is shown in parentheses.

[b] The concentration of [^{3}H]QNB is the mean from all experiments represented in the analysis (3.89 ± 0.27 nM, 22.4 ± 1.22 nM). The corresponding level of occupancy was calculated as [P]/([P] + K), with the value of K taken as 3.3 nM (Table S1).

[c] log K_2 − log K_1.

[d] The value is not well defined and was fixed at 1.